A perfusable encapsulation device housing stem cell derived pancreatic islets for diabetes cell therapy

By

Saleth Sidharthan Dharmaraj

Department of Chemical Engineering

McGill University

Montreal, Quebec, Canada

January 2025

A thesis submitted to McGill University in partial fulfillment of the requirements for the degree of Master of Science

Abstract

Type 1 diabetes (T1D) is an autoimmune disease characterized by the destruction of insulin-producing beta cells leading to insulin deficiency and chronic hyperglycemia. The current standard of care involves frequent insulin administration, which does not achieve the precise glucose regulation of functional beta cells. Consequently, there is a need for alternative, long-term therapeutic strategies to improve glycemic control. Islet transplantation is a promising treatment option where insulin-producing cells from organ donors are transplanted into recipients as allografts. However, this approach is limited by donor islet scarcity and the requirement for lifelong immunosuppression to prevent graft rejection. Encapsulation strategies have been developed to shield transplanted islets from immune attack using permselective polymer matrices, but diffusion-limited nutrient and oxygen transport often leads to graft cell loss and impaired function. Here, a device with embedded vascular channels is proposed to enhance transport of nutrients such as oxygen and secreted products such as insulin. Single-channel and multi-channel devices were fabricated using sacrificial sugar lattice 3D printing, polymer coating, and aseptic cell loading in alginate. *In vitro*, devices loaded with MIN6 beta cell lines demonstrated rapid insulin secretion in response to glucose stimulation, while devices with stem cell-derived islets (SC-islets) retained viability and function after 48 h of perfusion. Human-scale devices were then developed to evaluate safety and early human graft survival in pigs. The devices remained patent for one week with no adverse side effects during the acute phase post transplantation. Histological analysis confirmed the absence of thrombosis or fibrosis, and encapsulated SC-islets expressed maturation markers, including insulin and glucagon upon explant. This synergistic approach combining SC-islets with a perfusion-based device holds significant potential for advancing T1D treatment by supporting islet survival and function.

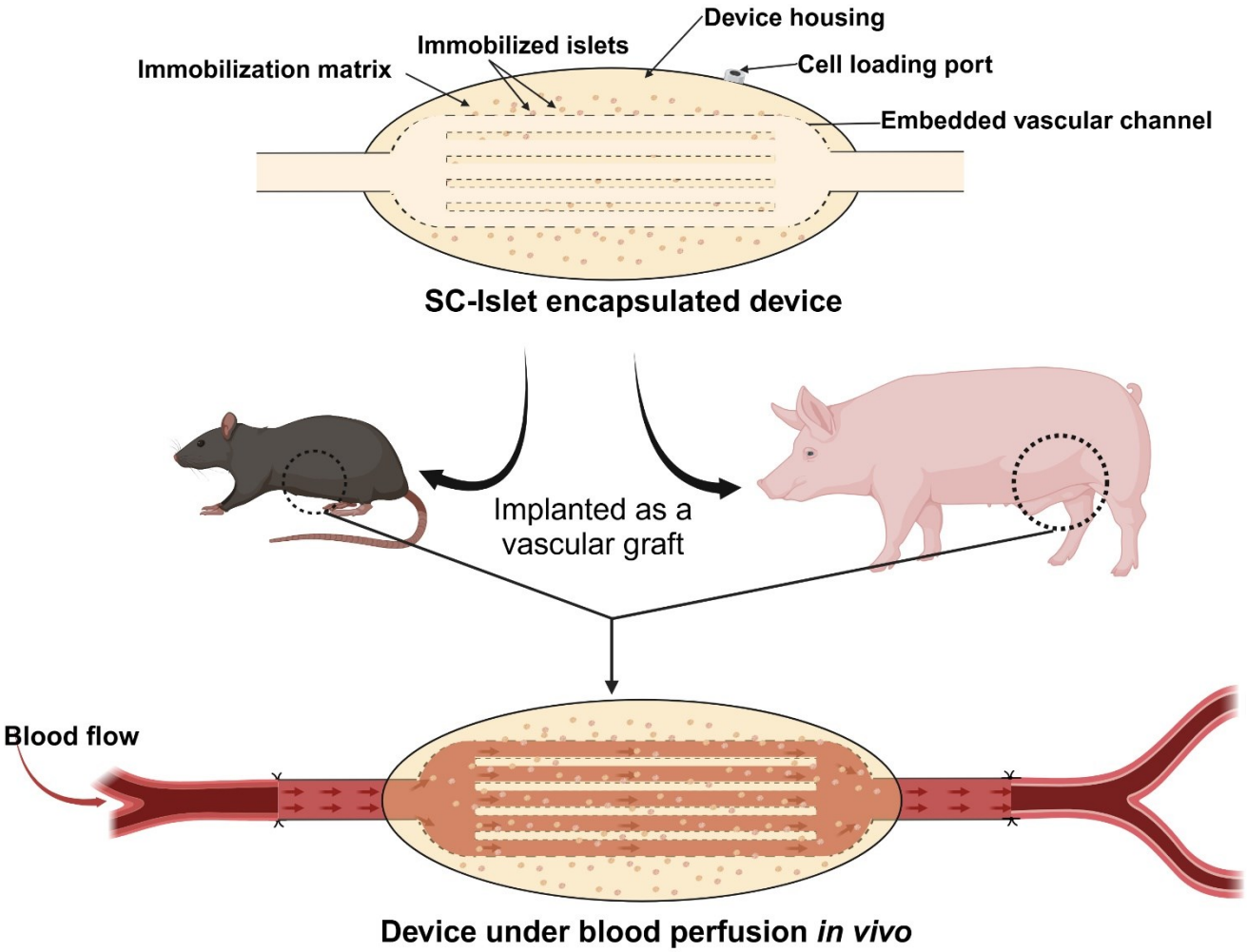

An illustration of the encapsulation device implanted and perfused *in vivo* (created using biorender.com)

Résumé

Le diabète de type 1 (DT1) est une maladie auto-immune caractérisée par la destruction des cellules bêta productrices d'insuline, entraînant une carence en insuline et une hyperglycémie chronique. L'approche thérapeutique actuelle repose sur l'administration fréquente d'insuline, ce qui ne permet pas d'atteindre la régulation glycémique raffinée atteinte par des cellules bêta fonctionnelles. Des stratégies thérapeutiques alternatives et durables pourraient significativement améliorer le traitement. La transplantation d'îlots pancréatiques, où des cellules produisant de l'insuline provenant d'un don d'organe sont infusés dans le foie de la personne diabétique, est une option prometteuse. Cependant, cette approche est limitée par la rareté des îlots disponibles et la nécessité d'une immunosuppression à vie pour prévenir le rejet du greffon. Des stratégies d'encapsulation ont été mises au point afin de protéger les îlots transplantés contre l'attaque immunitaire à l'aide de matrices polymériques de perméabilité sélective, mais le transport limité des nutriments et de l'oxygène par diffusion entraîne souvent une perte cellulaire et fonctionnelle des îlots greffés. Ici, un dispositif avec des canaux vasculaires intégrés est proposé pour améliorer le transport des nutriments, tels que l'oxygène, et des produits sécrétés, tels que l'insuline. Des dispositifs uni- ou multi-canaux sont d'abord fabriqués en imprimant des réseaux sacrificiels en sucre vitrifié qui sont revêtus d'un polymère avant de dissoudre le sucre et d'introduire des cellules dans une matrice d'alginate. *In vitro*, des cellules bêta de la lignée MIN6 cultivées dans le dispositif montrent une sécrétion rapide d'insuline en réponse à la stimulation par le glucose. Le dispositif permet aussi la survie d'îlots dérivés de cellules souches (îlots-CS) après 48 heures de culture sous perfusion. Des dispositifs conçus pour accueillir des doses d'îlots thérapeutiques chez l'humain ont ensuite été développés pour évaluer la sécurité des dispositifs dans un modèle porcin, ainsi que la survie à court terme d'îlots humains. Les dispositifs ont permis de maintenir un flux sanguin

pendant une semaine sans effets secondaires indésirables au cours de la phase aiguë post-transplantation. L'analyse histologique a confirmé l'absence de thrombose ou de fibrose, et les îlots-SC encapsulés ont exprimé des marqueurs de maturation, y compris l'insuline et le glucagon, après explantation. Cette approche synergique combinant des îlots-CS avec un dispositif de perfusion pourrait faire progresser le traitement du DT1.

Acknowledgements

I am deeply grateful for the immense support and encouragement I have received throughout my master's degree.

First and foremost, I extend my heartfelt gratitude to my supervisor, Prof. Corinne Hoesli, for welcoming me into her research group and for her exceptional guidance, patience and mentorship throughout my study. I am also thankful for the incredible opportunities she provided, enabling me to present my research at esteemed conferences and broaden my scientific perspective.

I would also like to express my sincere appreciation to all the members of the Hoesli Lab for their support throughout my research journey at McGill. A special acknowledgment goes to Lisa Danielczak for her efforts in managing the lab and making our lives easier. I am particularly grateful to Praveen Kumar and Hamid Orimi for their valuable discussions and insights on my project.

Beyond academia, I am profoundly thankful to my parents for their unwavering love, sacrifices and encouragement which have been my greatest source of strength. I also wish to extend my deepest gratitude to my dear friend Srividya Parthasarathy whose companionship and thoughtful advice have enriched both my academic and personal journey.

Table of contents

1. Chapter 1 16

1.1. Rationale 16

1.2. Objectives 17

2. Chapter 2 18

2.1. Literature review 18

2.1.1. Type 1 Diabetes 18

2.1.2. Limitations of Insulin Therapy and Islet Transplantation 19

2.1.3. Cell Sources for T1D Cell therapy 19

2.1.3.1. Primary Human Islets 19

2.1.3.2. Xenotransplants 20

2.1.3.3. Insulin producing cells from pluripotent stem cells 20

2.1.3.4. Genetically engineered SC-islets to reduce immunogenicity 22

2.1.4. Encapsulation to offer immunoprotection 23

2.1.4.1. Macroencapsulation 24

2.1.4.2. Microencapsulation 27

2.1.4.3. Nanoencapsulation 28

2.1.4.4. Perfusion enhanced encapsulation devices 30

2.1.5. Engineered Hydrogels to address encapsulation limitations 31

2.1.5.1. Immunomodulatory Hydrogels 32

2.1.6. Vascularizing the Islets 32

2.1.6.1. Angiogenesis via Co-Transplantation of Cells or Tissues 33

3. Chapter 3 36

3.1. Materials and Methods 36

3.1.1. Molding sacrificial sugar constructs 36

3.1.2. 3D printing sacrificial sugar constructs 36

3.1.3. Dip coating and Device fabrication 37

3.1.4. Scanning electron Microscopy 37

3.1.5. Immunostaining 38

3.1.6. Live/Dead staining 38

3.1.7. Dithizone staining 39

3.1.8. Histology 39

3.1.9. Cell Culture 39

3.1.10. hESCs differentiation to pancreatic lineage 40

3.1.11. Device perfusion *in vitro* in custom bioreactor 43

3.1.12. Dynamic Glucose-stimulated insulin secretion (GSIS) assay 45

3.1.13. *in vivo* Pig experiments 45

3.1.14. Statistical/graphical analysis and graphical generations 47

3.2. Results 48

3.2.1. Fabrication of Vascular networks 48

3.2.2. Perfusable encapsulation device fabrication 50

3.2.3. Device characterization 52

3.2.4. Device validation *in vitro* 54

3.2.4.1. MIN6 survival in rodent scale devices 55

3.2.4.2. SC-islet survival and glucose response in rodent scale devices 56

3.2.4.3. Human islets survival and glucose response in rodent scale devices 59

3.2.4.4. MIN6 survival and glucose response in single vs multichannel porcine scale devices 61

3.2.5. Device validation *in vivo* 64

4. Chapter 4 68

4.1. Discussion 68

4.2. Conclusion and future directions 73

5. References: 74

Preface

This thesis is written in the traditional monograph format. It contains Rationale and Objectives (Chapter 1), literature review (Chapter 2), materials and results (Chapter 3), Discussion, conclusion and future directions (Chapter 4).

Co-authored manuscript to be submitted

(A part of the results of this thesis is to be submitted as a part of another manuscript)

Engineering a vascularized and immunoprotective bioartificial pancreas for stem cell derived islet transplantation

Brassard JA*, **Sidharthan S**, Champion K, Wang H, Rioux Y, Lemaire F, Moeun B, Bates K, Wilts E, Kieffer T, Tchervenkov J, Soulez G, Leask RL, Bégin-Drolet A, Ruel J, Paraskevas S, Hoesli CA*

Manuscript to be submitted.

Contribution – My contributions for the manuscript to be submitted includes design and fabrication of human scale devices and conducting some of the *in vitro* experiments, modifying the device geometry and fabrication for *in vivo experiments,* assisting the surgeon during *in vivo* implantation and explant, processing the samples procured from the animal subjects for further analysis.

https://www.biorxiv.org/content/10.1101/2024.09.29.615298v1

Conference presentations

1) **Saleth Dharmaraj***, Jonathan Brassard, Jean Tchervenkov, Jean Ruel, André Bégin Drolet, Steven Paraskevas, Richard Leask, Marco Gasparrini, Corinne Hoesli. “A perfusable encapsulation device housing Stem cell derived pseudo-islets to treat type-1 diabetes”, 5th IPITA/HSCI/JDRF Summit. 2024, Boston, MA, USA. **(oral presentation)**
2) **Saleth Dharmaraj***, Jonathan Brassard, Jean Tchervenkov, Jean Ruel, André Bégin Drolet, Steven Paraskevas, Richard Leask, Marco Gasparrini, Corinne Hoesli. “Stem cell derived islets in a perfusable encapsulation device to treat type-1 diabetes”, Till and McCulloch meeting 2024, Montreal, QC, Canada. **(poster presentation)**
3) **Saleth Dharmaraj***, Jonathan Brassard, Jean Tchervenkov, Jean Ruel, André Bégin Drolet, Steven Paraskevas, Richard Leask, Marco Gasparrini, Corinne Hoesli. “A perfusable encapsulation device housing Stem cell derived islets for type-1 diabetes treatment”, Islet Study Group meeting 2023, Vancouver, BC, Canada **(poster presentation)**

Contributions of authors to the thesis monograph

- **Saleth Sidharthan Dharmaraj** – Contributed to the design and fabrication of rodent and human scale devices, conducted *in vitro* experiments with MIN6 and human islets, differentiated hESCs to SC-islets and performed *in vitro* experiments, modified and redesigned the devices for pig studies, assisted the surgeon during *in vivo* implantation and explant, processing the samples procured from the animal subjects for histological analysis, and wrote the manuscript.
- Jonathan Brassard – Helped in designing *in vivo* experiments, analyzing histology samples.
- Yannick Rioux – Optimized and printed sugar construct for the vascular network fabrication
- Hamid Orimi – Assisted in imaging for live/dead experiment
- Jean Tchervenkov – Performed the pig surgery
- Gilles Soulez – Performed doppler imaging and flow analysis during the pig experiments
- André Bégin-Drolet – Contributed to sugar printing
- Jean Ruel – Made the bioreactor for *in vitro* experiments
- Steven Paraskevas – Performed the pig surgery
- Daria Vdovenko – Imaged sections for histological analysis
- Corinne A. Hoesli – Contributed to the project ideation, secured funding, provided insights during the project and edited the manuscript

Note: C.H. and J.B. are co-founders of CellTerix Biomedical, a company aiming to commercialize devices for cellular therapy. The technology presented herein has been protected by a worldwide patent application (WO2024059942).

List of figures

Figure 3.1: (a) *In vitro* perfusion setup connecting the bioreactor to the peristaltic pump; (b) device connected between the perfusion loop inside the bioreactor 43

Figure 3.2: An An illustration of the vascular prosthesis fabrication process (created using biorender.com) 48

Figure 3.3: Representative images of fabricated vascular graft models; (a-c) 3D printed sugar lattices; (d-f) polymer coated sugar lattices' (g-i) polymeric vascular prosthesis post dissolution of sugar templates; scale bars – 2cm 49

Figure 3.4: An illustration of the encapsulation device fabrication with embedded channels (created using biorender.com) 50

Figure 3.5: Representative images of device fabrication process, 9-channel porcine scale device (a i-iv) and single channel rodent scale device (b i-iv); cutouts in (iv) displays the respective cross-section of the devices. 51

Figure 3.6: Scanning electron microscopy (SEM) images of (a-c) needle-coated vascular channel; (d-f) sugar-coated vascular channel and their respective cross sections and internal surface 53

Figure 3.7: (a) in vitro perfusion of rodent scale device in a makeshift bioreactor; (b) Live/Dead (Calcein/PI) imaging of MIN6 (10^8 cells/mL) embedded in alginate within the rodent scale device post 48hr perfusion (25mL/min), insert showing the cross-section of the cell laden alginate obtained from the device. 56

Figure 3.8: (a,d,e) Dithizone stained images of S7 SC-islets cultured in Device, suspension and Alginate slab respectively; (b) Laser confocal microscopic image of device cultured S7 SC-islets immunostained for maturation markers Insulin/Glucagon (Green/Red) and DAPI (Blue); (c,f,g)

Insulin response graphs of S7 SC-islets cultured in Device, suspension and Alginate slab respectively. 57

Figure 3.9: (a) Insulin response graphs of Human islets cultured in Device under perfusion; 5000-7000 islets per device, (b) suspension and (c) alginate slab 60

Figure 3.10: (a,b,c) Cross-section of the 9 channel device with MIN6 (10^8 cells/mL) embedded alginate, the respective Live/Dead (Calcein/PI) stained image and insulin response curve; (d,e) Live/Dead (Calcein/PI) stained image of single channel device with MIN6 (10^8 cells/mL) embedded alginate and the respective insulin response curve. 62

Figure 3.11: (a) Illustration of the intended device placement in porcine models (created using biorender.com); (b) Modified single channel porcine scale device; (c,d) representative images of Device and ePTFE control graft after implantation. 64

Figure 3.12: (a) Doppler ultrasound image of blood flow in the device before explanation; (b) Laser confocal microscopic image of in vivo device cultured S7 SC-islets immunostained for maturation markers Insulin/Glucagon (Green/Red) and DAPI (Blue); (c,f) representative images of device and ePTFE control graft post explant respectively; (c,f) H&E stained images of device and control graft sections respectively; (e,h) Massion's trichrome stained images of device and control graft sections respectively. 65

Figure 4.1: Immunoprotection and Vascularization Profiles of Notable Islet Encapsulation Devices 69

List of tables

Table 3.1: Differentiation media formulations 42

List of abbreviations

T1D	Type 1 diabetes
MIN6	Mouse insulinoma 6 cell line
SC-islets	Stem cell derived islets
3D	Three dimensional
PU	Polycarbonate polyurethane
SEM	Scanning electron microscopy
PBS	Phosphate buffered saline
DMEM	Dulbecco's Modified Eagle Medium
hESCs	Human embryonic stem cells
CMRL	Connaught Medical Research Laboratories
HEPES	4-(2-hydroxyethyl)-1-piperazineethanesulfonic acid
DMF	Dimethylformamide
GSIS	Glucose stimulated insulin secretion
ePTFE	Expanded polytetrafluoroethylene

1. Chapter 1

1.1. Rationale

Type 1 diabetes (T1D) is an autoimmune disease that affects millions worldwide, including over 300,000 Canadians. This chronic condition is caused by the immune-mediated destruction of insulin-producing beta cells in the pancreas leading to lifelong reliance on exogenous insulin to manage blood glucose levels. Despite advancements in insulin delivery technologies, these methods fail to replicate the precise glucose regulation of healthy pancreatic tissues. Pancreatic islet transplantation has demonstrated success in restoring insulin independence and improving glycemic control. However, this approach is limited by the scarcity of donor islets and the requirement for lifelong immunosuppression to prevent graft rejection, which increases infection risks and other adverse effects. Encapsulation of islets within a biomaterial matrix has emerged as a potential solution thus providing a protective barrier against immune system while permitting nutrient and oxygen exchange. However, current encapsulation methods face challenges, including diffusion-limited mass transfer constraints due to delayed or insufficient graft vascularization, and cell death further compromising graft viability and function. To address these limitations, this project focuses on developing a perfusion-based encapsulation device with embedded vascular channels to improve mass transfer and promote graft survival. A scaled-down prototype of this device is optimized for rodent models intended for preclinical validation. Ideally, these vascular lattice devices aim to provide immunoprotection while facilitating immediate vascularization to meet the metabolic demands of encapsulated cells. By combining encapsulation strategies with vascular integration, this approach has the potential to enhance graft survival and function, advancing cell-based therapies for T1D.

1.2. Objectives

The objective of this project was to develop an islet encapsulation that would provide immunoprotection from the host's immune system by encapsulating the cells within a non-biodegradable hydrogel while also providing immediate vascularization by embedded vascular channels within the device which could be irrigated immediately when implanted as a vascular graft.

The specific objectives are to:

1. Design and fabricate rodent scale and porcine scale macroencapsulation devices with embedded vascular channels within them.
2. Validate the performance of the vascular lattice devices *in vitro* by encapsulating insulin producing cell lines and SC-islets and assessing the survival and function of these cells while within the device under perfusion.
3. Demonstrate preliminary safety of devices as vascular graft implants, and proof-of-concept of cell survival *in vivo*.

2. Chapter 2

2.1. Literature review

2.1.1. Type 1 Diabetes

T1D is a chronic autoimmune disease characterized by the destruction of insulin-producing beta cells in the pancreas, leading to insulin deficiency. It affects millions of individuals worldwide and poses significant health and economic challenges. The prevalence of T1D has been steadily increasing particularly among children and young adults [1] The pathophysiology of T1D involves a complex interplay of genetic, environmental, and immunological factors. While the precise triggers of this response remain unclear, viral infections, dietary factors, and cellular stress could play a role in triggering autoimmunity in genetically predisposed individuals [2].

In the early stages of T1D, patients are typically asymptomatic however, circulating autoantibodies against beta-cell antigens can often be detected. As the disease progresses, the immune response intensifies targeting beta cells more aggressively. Animal studies estimate that clinical symptoms of T1D manifest after approximately 80% reduction in beta-cell mass [3]. This beta-cell loss results in insulin deficiency, disrupting glucose regulation and causing hyperglycemia. Insulin is essential for blood glucose regulation as it facilitates glucose uptake. Without sufficient insulin, glucose transport is impaired, leading to elevated blood glucose levels. Persistent hyperglycemia can result in severe complications, including vascular and nerve damage, increased risks of cardiovascular diseases, renal failure, and blindness. Despite advancements in understanding the mechanisms of T1D, the precise factors driving beta-cell autoimmunity remain elusive [1, 4].

2.1.2. Limitations of Insulin Therapy and Islet Transplantation

The primary treatment for T1D is lifelong insulin therapy, which requires daily blood glucose monitoring and insulin administration to achieve glycemic control. However, insulin therapy has inherent limitations including risks associated both with hypoglycemia which can be life-threatening, and hyperglycemia leading to long-term complications such as cardiovascular disease and nephropathy. Pancreatic islet transplantation has emerged as an alternative strategy to restore endogenous insulin production. While promising, this approach is constrained by several challenges, including limited donor availability, the need for lifelong immunosuppression, and ensuring long-term graft survival [5]. Despite improvements in islet isolation techniques and immunosuppressive protocols, the widespread application of islet transplantation remains hindered by the above-mentioned limitations. Furthermore, recent studies indicate that even with advancements in promoting graft viability, achieving consistent glycemic independence remains challenging [6].

2.1.3. Cell Sources for T1D Cell therapy

2.1.3.1. Primary Human Islets

Current islet transplantation practices primarily depend on human islets isolated from deceased donors. The isolation process involves enzymatic digestion and density gradient centrifugation to extract islets, followed by a short culture period to remove apoptotic cells and ensure quality before transplantation [7]. However, human islets comprise only 1-2% of the pancreas, resulting in severely limited supply. This scarcity allows treatment for less than 1% of the type 1 diabetic population [8]. In addition, the functional variability of islets among donors can impact transplant outcomes, while donor shortages introduce ethical challenges regarding organ

allocation. Addressing these limitations requires the exploration of alternative sources and innovative strategies to replace primary human islets.

2.1.3.2. Xenotransplants

Due to the similarity to human insulin, porcine insulin which differs only by one amino acid was one of the first to be used for T1D treatment. Early studies demonstrated functional grafts of porcine islets showing survival in patients up to a year post-transplant. A major challenge in porcine islet xenotransplantation is the immune response to porcine antigens like galactose-α1,3-galactose (Gal) and N-glycolyl neuraminic acid (Neu5Gc). While previous attempts at removing anti-Gal antibodies only delayed rejection, genetic modifications in pigs to delete Gal and Neu5Gc significantly reduced antibody binding [9]. Pigs with these modifications had improved compatibility compared to other species. Yet, transmission of porcine endogenous retroviruses (PERVs) remains a concern, although advances in genetic engineering have inactivated retroviruses and enhanced the safety of porcine transplants [10]. Studies using immunosuppressive regimens in nonhuman primates (NHPs) showed porcine islet grafts maintained normoglycemia for over six months with some lasting nearly two years [11]. Recent milestones, including the first pig-to-human heart transplant using genetically engineered pigs, further validate the potential of porcine islet xenotransplantation [12].

2.1.3.3. Insulin producing cells from pluripotent stem cells

Embryonic stem cells (ESCs) have emerged as a primary source for generating insulin-producing cells due to their distinct characteristics [13]. Derived from the inner cell mass of a blastocyst and cultured *in vitro*, ESCs possess an unlimited capacity for self-renewal attributed to their high telomerase activity, as well as the ability to differentiate into various cell lineages,

including pancreatic beta cells [14, 15]. When appropriately directed, they can differentiate into multiple islet cell types, demonstrating significant potential for beta-cell replacement therapies [16]. Several preclinical studies have highlighted the potential of ESC-derived insulin producing beta cells in diabetes treatment. Early experiments demonstrated that beta cells derived from ESCs transplanted into diabetic mice could secrete insulin in response to glucose stimulation and regulate blood glucose levels [14]. More recent studies have shown that human ESC-derived beta cells exhibit glucose-responsive insulin production *in vitro* similar to endogenous islets. When encapsulated and transplanted into diabetic mice, these cells effectively controlled blood glucose levels and reduced inflammatory markers, such as IL-1 expression [15, 16].

Owing to the ethical concerns in using human embryos sourced ESCs, induced pluripotent stem cells (iPSCs) have gained prominence as a viable source for generating functional beta cells – both for transplantation into many recipients as allografts, or for autologous transplants. The advantages of autologous grafts are limited in the case of type 1 diabetes because of autoimmune responses, but this strategy can be of significant interest if autoimmune rejection can be countered or in non-autoimmune diabetes [17]. Insulin-producing islet-like cell clusters (SC-islets) can be produced from several iPSC lines [18-20]. Wang et al. demonstrated that patient-derived mesenchymal stromal cells obtained from adipose tissues, when reprogrammed to bestow pluripotency can be differentiated into pancreatic beta cells and transplanted back into the same individuals, showcasing the feasibility of autologous cell therapy for diabetes. They also showcased their results from phase I clinical trials in humans with promising outcomes [21].

Despite their potential, the pluripotent nature of these cells poses significant risks, particularly their tendency to form teratomas or teratocarcinomas which could be due to

chromosomal aberrations accumulated during repeated cell replication cycles [22]. In addition, preclinical studies have reported the formation of tumors in mice following transplantation of ESC-derived beta cells into the kidney capsule or spleen, despite temporary improvements in hyperglycemia [14]. The U.S. Food and Drug Administration (FDA) recently eased its requirements for hESC-derived cells to be transplanted in removable devices in case teratomas develop. For instance, Vertex Pharmaceuticals have been conducting clinical trials with their VX-880 where unprotected hESCs derived islet progenitors are transplanted into the portal vein of individuals with T1D, but they had to pause their studies due to unrelated patient deaths and they have resumed their studies recently [23].

2.1.3.4. Genetically engineered SC-islets to reduce immunogenicity

While undifferentiated human pluripotent stem cells (hPSCs) maintain some immune privilege, their differentiation increases their visibility to the immune system. As stem cells differentiate into pancreatic lineage cells, major histocompatibility complex (MHC) class I expression is upregulated. SC-islets predominantly express human leukocyte antigen (HLA) Class I antigens, raising the risk of alloimmune rejection [24, 25]. Recent studies have focused on using genetic modifications to enhance the survival of SC-islets in transplantation settings. Beta-2-Microglobulin is a small protein that forms a component of MHC class I molecules and it is involved in the stable expression and surface presentation of MHC class I molecules on the cells. Beta-2-Microglobulin knock-out SC-islets prevents MHC class I formation and has been shown to reduce T cell activation [26]. Programmed Cell Death Ligand 1 (PD-L1) is an immune checkpoint molecule expressed on the surface of various cell types, including SC-islets and it plays a key role in suppressing the immune response by binding to PD-1 receptor on T cells thereby

inhibiting T cell activation and promoting immune tolerance. *Yoshihara et al* [25] demonstrated that overexpression of PD-L1 has improved SC-islets functionality and protected against alloimmune recognition in humanized mouse models.

2.1.4. Encapsulation to offer immunoprotection

The concept of encapsulation was introduced in 1933 when xenotransplantation of human insulinoma tissue using membranous bags was first tested in rats [27]. The field of immune-isolated transplantation gained significant traction in the early 1950s through experiments that tested the survival of allotransplanted tissue in an extravascular space with and without an encapsulating membrane. These studies demonstrated that the encapsulating membrane prevented immune cell contact, thereby avoiding the direct antigen presentation pathway and prolonging the survival of non-vascularized tissue, even though mass transfer was limited. Additionally, encapsulation may also reduce indirect antigen presentation by limiting the release of donor antigens that could be processed by host antigen-presenting cells [28], although this effect depends on the permeability and degradation properties of the membrane.

Encapsulation devices have emerged as a promising approach to overcoming the challenges of islet transplantation by providing a physical barrier between transplanted β-cells and their recipients, thus eliminating the need for immunosuppressive drugs. Most encapsulation devices designed to be immunoprotective rely on creating a physical size exclusion barrier between the graft and the host, aiming to provide nutrient, waste and transport of smaller proteins such as insulin, while excluding larger components such as cells and potentially antibodies [29]. For an immunoprotective encapsulation device to be effective, it must achieve key criteria such as ensuring an adequate blood supply for the islet survival and function, exhibit appropriate insulin

and glucose kinetics to maintain normoglycaemia, being biocompatible, serve as an immune barrier to prevent rejection, and prevent the escape of embedded cells to contain any potentially tumorigenic cells. These features are critical to ensuring that β-cells are protected, functional, and able to respond appropriately to changes in blood glucose levels [30].

Over the past few decades, various macroencapsulation, microencapsulation and nanoencapsulation techniques have been developed to create immunoprotected β-cells [31]. Micro/nanoencapsulation involves the use of small capsules or coatings (micro-nanometer size range) containing a single cell or islet aimed to optimize the surface area-to-volume ratio to improve nutrient exchange. However, they have significant limitations such as difficulty controlling membrane thickness and pore size, the need for hundreds of thousands of individual microcapsules or nanoencapsulated islets per recipient in humans, and challenges in recovering and tracking of individual capsules. On the other hand, macroencapsulation devices house multiple cells or islets in a single larger device, allowing for better control over membrane properties such as pore size [32, 33]. Studies over the recent years have focused on addressing the challenges of various encapsulation strategies by improving the encapsulation material, optimizing the transplantation site, refining device configurations, and enhancing vascularization and immune modulation.

2.1.4.1. Macroencapsulation

Macroencapsulation systems generally involve encapsulating a bulk concentration of cells usually in a device of circular or planar geometry. The Islet Sheet developed by Islet Sheet Medical, a planar flat-sheet device featuring a multilayered construct of alginate. The central layer contains islets, and external acellular alginate layers provide immunoprotection. This device

demonstrated excellent graft survival, maintaining normoglycemia in diabetic dogs for 12 weeks [34]. Another planar device, the monolayer cellular device incorporates a collagen matrix embedded with islets and covered by two alginate layers. When tested in diabetic monkeys, this device corrected hyperglycemia for up to six months without immunosuppression, withstanding strong immune responses while demonstrating impermeability to IgG for up to 20 weeks [35]. TheraCyte is another notable islet encapsulation device that incorporated an outer Teflon-based membrane to provide mechanical strength and promote capillary ingrowth. The inner membrane was a semipermeable hydrogel membrane, providing immune protection. Although they showed initial success in clinical trials, the device faced significant cell loss due to inadequate oxygenation and difficulty in device retrieval [36]. The company ViaCyte developed PEC-Encap and PEC-Direct to address immunoprotection and vascularization limitations in islet encapsulation. PEC-Encap encapsulates PEC-01 cells derived from embryonic stem cells within a PTFE immunoprotective chamber. Once implanted, the cells differentiate into glucose-responsive, insulin-producing β cells and stimulate angiogenesis to enhance blood vessel formation in the surrounding tissue. From the Phase I/II clinical trials for PEC-Encap commenced in 2014, and by 2018, ViaCyte reported that the device demonstrated safety and tolerance in patients [37]. PEC-Direct is an improved version of PEC-Encap, designed to enhance vascular ingrowth but lacking inherent immunoprotection. Clinical trials for PEC-Direct are focused on evaluating its ability to provide functional β-cell replacement for T1D patients while promoting better vascularization [38]. MailPan® is another encapsulation aimed to address the vascularization and islet survival issue. It consists of a circular flat pouch made of semi-permeable membranes that allow selective exchange of molecules, such as insulin, glucose, and oxygen, while efficiently rejecting larger molecules like human IgG. The device also has an entry/exit injection port, allowing for easy cell

replacement without requiring device retrieval. The device exhibited minimal immune response in rats although the blood glucose normalization was suboptimal, and the device faced significant cell loss due to inadequate oxygenation [39].

One of the primary challenges of macroencapsulation devices is the limited oxygen diffusion through the semipermeable membrane, compromising islet viability, insulin secretion and potentially leading to graft failure. The ß-Air device by Beta-O_2 Technologies addresses this issue with an oxygen-refueling system. This device consists of a semipermeable chamber containing islets in an alginate hydrogel and an additional compartment for daily oxygen supply through an external tubing system. The ß-Air device has shown promise in animal studies, preserving the function of encapsulated islets and maintaining normoglycemia in diabetic pigs for several months yet in human trials, the therapeutic impact was suboptimal likely due to fibrosis as the islets survived but the secreted insulin didn't reach the circulation. [40, 41]. Additionally, strategies incorporating oxygen carriers such as perfluorocarbons or calcium peroxide within hydrogels have demonstrated improved cell viability and metabolic activity *in vitro*, suggesting potential for overcoming oxygen limitations [42].

The BioHub system, developed by the Diabetes Research Institute of Miami, takes a different approach to enhance graft vascularization and improving oxygenation. It uses an injectable hydrogel-like matrix derived from the patient's plasma and thrombin to encapsulate islets. The matrix degrades over time, facilitating blood vessel formation around the islets. In diabetic monkeys, allogeneic islets encapsulated in the BioHub system and implanted in the omentum resulted in reduced insulin dependence and well-preserved islet morphology with extensive vascularization [43]. Although their pre-clinical studies were successful in islet

engraftment and function, they were not immunoprotected requiring long-term immunosuppression. Other devices such as the 'thread-reinforced alginate fiber for islet encapsulation' have also been developed to improve diffusion properties, retrievability and scalability. The device demonstrated normoglycemia in diabetic mice and retrievability in dogs, highlighting its versatility and immune protection capabilities [44].

The primary advantage of macroencapsulation systems lies in their retrievability and the ability to implant islets precisely in a single location. Embedding islets within hydrogels prevents aggregation, maintains morphology, and enhances oxygen and nutrient supply, improving viability and survival. Despite promising preclinical outcomes, clinical trials of macroencapsulation devices remain limited. Challenges such as limited oxygen diffusion, insulin kinetics and the structural integrity of certain hydrogels must be addressed to ensure long-term functionality.

2.1.4.2. Microencapsulation

Microencapsulation involves embedding single cells or aggregates within micron scale capsules made from hydrogels such as alginate, which is favored due to its biocompatibility and ease of gel formation. Alginate beads are often coated with cationic polymers such as poly-L-lysine (PLL) or poly-L-ornithine (PLO) to improve stability and reduce permeability to antibodies, followed by additional alginate coatings to avoid exposure of cationic polymers which trigger immune reactions [45]. Alternative approaches, such as barium-cross-linked alginate capsules, have demonstrated reduced immunogenicity [46]. Pre-clinical studies using xenogeneic islets encapsulated in such materials have shown encouraging results in reducing insulin dependence in rodents and non-human primates restoring glycemic control for a prolonged time period [47].

Several clinical trials have demonstrated the feasibility of microencapsulation in diabetes treatment. Early studies using alginate-poly-L-lysine-alginate microcapsules reported insulin independence in diabetic patients for several months, yet issues such as fibrotic reactions limited success [45] Later trials using improved formulations like magnetically purified microcapsules achieved better outcomes in both animal models and pilot human studies [48, 49]. Xenotransplantation of porcine islets encapsulated in alginate microcapsules has also shown potential for clinical application [50].

Compared to macroencapsulation, microencapsulation provides superior oxygen and nutrient diffusion due to its high surface-area-to-volume ratio, enhancing cell viability and function. Smaller device sizes enable minimally invasive implantation. In addition, failure of individual microcapsules does not compromise the entire graft which is a significant advantage over macroencapsulation systems [51]. Despite these advantages, microencapsulation faces challenges in scalability and clinical translation. Large-scale encapsulation methods can cause hypoxic stress, and the high volume of empty capsules in transplant material may provoke immune responses and removing the cell free capsules is time and labor intensive [52].

2.1.4.3. Nanoencapsulation

Nanoencapsulation is the process of creating nanometer-scale hydrogel coatings around islets to provide immunoisolation while maintaining essential nutrient and oxygen exchange, ultimately improving graft function and viability [31, 53]. Nanoencapsulation relies on interfacial polymerization methods, such as visible light-initiated thiol-norbornene polymerization which form conformal hydrogel coatings on islet surfaces. Eosin Y, a biocompatible photoinitiator facilitates the crosslinking of acrylated polyethylene glycol (PEG) under visible light resulting in

a uniform, nano-thin barrier that protects islets from immune rejection [53, 54]. PEG hydrogels are particularly advantageous due to their high permeability, low immunogenicity, and tunable mechanical properties which allow optimization for specific transplantation settings. Alternative materials including alginate and poly-L-lysine, have also been explored for their potential in nanoencapsulation. While alginate-based systems are well-established for microencapsulation, modifications to alginate chemistry or multi-polymer layered coatings have improved its applicability to nanoencapsulation enhancing mechanical stability and biocompatibility [55, 56]. Advances in multi-layer coatings, such as layer-by-layer assembly of nano-thin PEG films, have demonstrated enhanced islet protection and reduced fibrotic responses in preclinical tests. [57]. Nanolayer-coated islets have also exhibited sustained insulin secretion, long-term viability, and protection from immune-mediated destruction without the need for systemic immunosuppression. Further, studies have demonstrated the ability of nanoencapsulated islets to maintain normoglycemia in diabetic animal models for extended periods [58].

Advances in nanoencapsulation technology had potentially addressed several limiting factors of macro and microencapsulation strategies including hypoxia-induced cell death and delayed insulin kinetics. For instance, the reduction in capsule thickness minimizes diffusion barriers, ensuring better oxygen and nutrient exchange while maintaining immunoprotection. The primary concern with nanoencapsulation is ensuring consistent and reproducible coating thickness and uniformity across large-scale islet populations. Additionally, the long-term structural integrity of the coating remains uncertain, as islets undergo remodeling post-transplantation, which may impact the stability and functionality of the encapsulation. Advances in material science and fabrication techniques, such as automated coating and photopolymerization systems could further streamline this process and mitigate the limitations.

2.1.4.4. Perfusion enhanced encapsulation devices

Encapsulation strategies utilizing active blood perfusion aim to enhance mass transport efficiency through convective flow rather than passive diffusion, addressing a key limitation of conventional diffusion-based systems. Early developments in this field were the development of arteriovenous shunt-based devices by Monaco *et al*. [59]. These systems incorporated a selectively permeable acrylic membrane housed within a rigid casing, connected to a polytetrafluoroethylene vascular graft, allowing direct perfusion of encapsulated islets. While these devices successfully restored glycemic control in pancreatectomized dogs, they ultimately failed due to thrombosis, membrane collapse, and loss of vascular connection, highlighting the challenges of long-term vascular integration. Further, the first successful use of a perfused vascular device was in alloxan-induced diabetic rats. Utilizing Amicon XM-50 hollow fibers composed of polyacrylonitrile-polyvinyl chloride copolymer, this system enabled glucose-responsive insulin secretion. However, the small internal diameter of these fibers led to thrombosis and necessitated chronic systemic anticoagulation, restricting *in vivo* applicability. Subsequent iterations employed larger bore devices which exhibited improved patency in non-heparinized canine models for up to seven weeks, maintaining appropriate glucose-stimulated insulin release [60]. To enhance hemocompatibility and vascular integration, Shuvo Roy's laboratory developed an AV shunt device utilizing a silicon nanopore membrane, designed to facilitate ultrafiltration while minimizing direct immune cell interactions [61]. Jeff Karp's Geometrically Refined and Accessible Cell Encapsulation system presents a different approach, integrating pre-vascularized channels within an immune-isolating scaffold to promote host vascularization post-implantation, thereby enhancing mass transport [62]. Further, devices like iBAP [63] and Humacyte™

biovascular pancreas [64] are also under development to enhance mass transfer to the islets via convective flow.

Despite their potential, perfusion enhanced devices face several challenges that hinder clinical translation. The primary concern is thrombosis, as direct blood contact leads to clot formation potentially leading to embolism thus requiring chronic anticoagulants. Intervascular surgical implantation is often invasive and poses risks such as vascular injury, infection, and impaired blood flow. Mechanical failure of the device is a major concern that compromise device function and pose serious health problems such as ischemia. Additionally, Immune responses, such as fibrosis reduce mass transport efficiency and long-term functionality as fibrotic encapsulation restricts glucose and insulin diffusion. Further, these vascular devices divert a major volume of blood flow from native vessels which could cause cardiac stress on patients with pre-existing conditions. Hence, a perfusion-based encapsulation device that overcome these issues would be an ideal candidate for clinical translation.

2.1.5. Engineered Hydrogels to address encapsulation limitations

Although encapsulation strategies show significant breakthroughs, these strategies still suffer from the severe drawbacks which are insufficient vascularization for the islet, activation of the host's immune response which both can lead to graft rejection and reduced functionality of the encapsulated islets. To overcome these challenges, various strategies have been investigated such as incorporation of angiogenic factors to promote vascularization or co-encapsulation of immunoprotective agents.

2.1.5.1. Immunomodulatory Hydrogels

Chemical modifications of hydrogel structures are an effective approach to achieve immunomodulation. Alginate-based hydrogels, widely used for islet encapsulation can be modified to resist fibrotic tissue formation and reduce foreign body responses. For instance, the addition of zwitterionic polymers to alginate hydrogels has been demonstrated to reduce protein adsorption, minimize macrophage activation, and decrease fibrosis, thus improving graft longevity [65]. Recent studies include integrating carboxy betaine-based polymers or phosphorylcholine-conjugated materials, which have shown to suppress foreign body responses effectively. Modifying mechanical properties such as stiffness, density etc. also play a role in immune modulation. Hydrogels with optimized stiffness not only reduce host immune reactions but also create an optimal environment for islet survival and insulin secretion [65].

2.1.6. Vascularizing the Islets

Islets are highly vascularized tissues, and such dense vascularization is vital for their function, particularly in blood glucose regulation and insulin secretion. Mimicking this feature of a native islet is one of the major shortcomings of encapsulation technologies. Vascularization relies on endothelial cells lining the blood vessels and is facilitated by VEGF-A binding to VEGF receptors VEGFR-1 and VEGFR-2. These receptors play crucial roles in vasculogenesis, angiogenesis, vascular permeability, and the formation of endothelial fenestrations [66]. In addition, during embryonic development, endothelial-endocrine cell interactions and vascular remodeling significantly contribute to pancreatic morphogenesis [67]. Following islet isolation and transplantation, reestablishing blood flow to the grafted islets is significantly delayed and without sufficient oxygen and nutrients, transplanted islets experience hypoxia and necrosis. Long-

term survival of these islets depends on robust vascularization, which supports cell viability and insulin secretion. Strategies like co-transplantation of supportive cells have shown promise in enhancing vascular formation at the implantation site [29].

2.1.6.1. Angiogenesis via Co-Transplantation of Cells or Tissues

Co-encapsulation of islets with angiogenic or regulatory cells has demonstrated improved outcomes in terms of islet survival and function. Regulatory T cells, which modulate immune responses and promote angiogenesis, are a notable example. These cells, characterized by CD4, CD25 and FOXP3 expression have been used successfully in islet transplantation, and been shown to preserve islet population post transplantation [68]. Multipotent adult progenitor cells (MAPCs) and mesenchymal stromal cells (MSCs) are also being studied for co-transplantation. MAPCs suppress immune cells and enhance angiogenic responses while MSCs secrete immunosuppressive molecules like prostaglandin E2, reduce hypoxia, and inhibit immune cells such as NK cells, macrophages, and T cells [69]. MSCs, typically derived from bone marrow or adipose tissue are particularly effective, promoting islet viability and insulin secretion post-transplantation. For instance, co-transplantation of MSCs with islets in mice resulted in normoglycemia alongside improved endothelial cell numbers within the graft [70]. Endothelial cells are another promising option, as they maintain essential signaling between β-cells and enhance insulin release. Studies have demonstrated increased insulin secretion when β-cells are co-cultured with endothelial cells, highlighting their role in preserving islet function and viability [71]. While co-encapsulation with angiogenic and regulatory cells enhances islet survival and function, the process of host vascular integration is inherently slow, delaying the formation of functional microvasculature within the graft. To overcome this delay in vascularization, preformed micro vessels (MV) obtained from

adipose tissues were co-transplanted with islets. Ideally, MVs derived from recipient's adipose tissue could be utilized to prevent immune rejection. The immediate vascularization offered by MVs where beneficial when human islets transplanted with MV achieved normoglycemia immediately. Additionally, MV transplantation restores the intra-islet microvascular network that is disrupted during islet isolation, improving oxygenation and nutrient delivery within the graft and thereby enhancing islet survival and insulin secretion. Another key advantage is the reduction in the required islet mass for achieving glycemic control, which is critical given the scarcity of donor pancreases [72, 73]. Despite the advantages of MV-based vascularization, there are several limitations to consider. MV from diabetic donors may experience delayed inosculation, potentially impairing vascularization in hyperglycemic hosts. Long-term stability and functionality of MV-induced vessels, including resistance to thrombosis, remain uncertain.

Chapter 2 aimed to offer a thorough exploration of the evolving landscape of T1D therapies, with a particular emphasis on the inherent limitations in traditional insulin therapies, islet transplantation, and cell encapsulation techniques. Although islet transplantation shows prominent potential, significant challenges remain, such as immune rejection, long-term graft survival, and the optimization of graft function post-transplantation. While encapsulation strategies provide vital immunoprotection, they still struggle to ensure adequate vascularization and nutrient diffusion, the two crucial factors for maintaining cell viability and enabling insulin secretion. To overcome these challenges, the development of convection-enhanced encapsulation devices presents a promising solution. These devices would offer a combination of a high surface area for efficient nutrient and oxygen exchange while also facilitating the active perfusion of encapsulated cells. This approach would not only promote cell survival but also ensure the delivery

of therapeutic doses of cells while preserving immunoprotection, addressing both the functional and long-term viability concerns that currently limit existing strategies.

3. Chapter 3

3.1. Materials and Methods

3.1.1. Molding sacrificial sugar constructs

Plastic molds were designed using AutoCAD (Autodesk) and fabricated using a TAZ Workhorse 3D printer (LulzBot) with Cura LE v3.6 software and PolyLite PLA filament (Polymaker). Polydimethylsiloxane (PDMS, Dow Chemical Company) was prepared by mixing the elastomer and curing agent at a 10% v/v ratio and cast over the plastic molds to create inverted molds for sugar templates. The PDMS was cured overnight in an oven at 60°C. To prepare the sugar glass mixture, 113 g of sucrose (Fisher) and 75 mL of distilled water were combined in a 500 mL beaker and heated on a digital hotplate stirrer with a feedback temperature control system (Scilogex, MS7-H550-Pro) The solution was stirred at 330 rpm using a 1-inch magnetic stir bar until the mixture reached 175°C. The molten sugar solution was then poured into preheated (75°C) PDMS molds and allowed to solidify at room temperature for 20–30 min before being demolded. Any minor imperfections in the sugar constructs were carefully polished off with a sharp scalpel.

3.1.2. 3D printing sacrificial sugar constructs

The 3D printing process for 9-channel sugar templates involved preparing a molten carbohydrate ink by dissolving 78 g of sucrose in 50 mL of water. This mixture was loaded into 20-mL glass syringes (Fortuna Brand) and inserted into a modified Airwolf AW3D XL printer, fitted with a custom print head and dual cooling air jets (7.5 PSI) positioned on either side of the nozzle. To ensure optimal printability, minimize caramelization, and facilitate rapid solidification, the printing parameters were carefully set to a 2.0 mm extrusion nozzle size, a volumetric flow rate of 0.123 g/min, a translational speed of 15 mm/min, and temperatures of 92°C for the print

head and 85°C for the nozzle. Custom G-code was used to fabricate the sacrificial sugar network, with each 9-branch channel requiring 80 min to print. A single sugar ink preparation yielded three templates. The printed structures were stored at 4°C in airtight packaging with silica gel to prevent moisture absorption and were transported from Québec to Montreal (a 3-h drive).

3.1.3. Dip coating and Device fabrication

The 3D printed/molded sugar constructs (for single channel and 9 channel human-scale prototypes) or 20G blunt head syringe needles (McMaster-Carr; for rodent scale prototypes), were dip-coated in a polycarbonate polyurethane (PU) solution consisting of 40 mL of Chronoflex AR 22% (AdvanceSource - 3100003-H), 25 mL of N,N-dimethylformamide (DMF, Sigma-Aldrich), and 12.93 g of sodium chloride crystals of size >45μm (NaCl, Sigma). For coating optimization, the salt concentration was adjusted to achieve NaCl-to-polymer weight ratios of 1:2, 2:2, and 3:2, while maintaining a constant DMF-to-Chronoflex ratio. Each sugar structure/needle underwent 3 to 5 dip-coating cycles, with a 2-h drying interval between coatings. After the final coating, the structures were dried over night at room temperature inside a fume hood. Once dried, the structures were immersed in reverse osmosis water to dissolve the sugar template and salt. For device fabrication, the coated sugar networks/needles were positioned within a two-piece PDMS mold designed to shape the external pouch. The external pouch was coated using the same dip-coating method described above. The sugar molds were coated three times with the polymer-salt mixture and a final dip coating was applied using a polymer solution without added salt, creating a smooth surface and sealing the device from leakages.

3.1.4. Scanning electron Microscopy

The graft structure was examined using a variable pressure scanning electron microscope (VP-SEM, Hitachi SU-3500). Prior to imaging, the grafts were dehydrated my immersing in

ethanol for 2 h and air drying overnight. The dried grafts were sectioned into 0.25 cm × 0.25 cm pieces to expose the internal surface. Imaging was performed at a pressure of 40 Pa, with an accelerating voltage ranging from 4 to 10 kV, depending on the desired magnification.

3.1.5. Immunostaining

The cell aggregates were rinsed twice with phosphate buffered saline (PBS) and fixed in 4% paraformaldehyde (Thermo Fisher Scientific) prepared in PBS for 15–20 min at room temperature. After fixation, tissues were permeabilized using 0.2% Triton X-100 in PBS for 1 h at room temperature followed by blocking with a protein block solution (Dako) for 3 h at room temperature. They were then incubated overnight at 4°C in an antibody diluent solution (Dako) containing the primary antibody against humans (Insulin: rabbit-anti-human; Clone C27C9; Cell Signalling, Glucagon: mouse-anti-human; Clone U16-850; Sigma Aldrich). After incubation, they were washed every one h for 3 h with PBS at room temperature and incubated overnight at 4°C with a secondary antibody (Alexa 647 donkey-anti-rabbit; 1:500 in antibody diluent or Alexa 647 donkey-anti-mouse; 1:500 in antibody diluent; Thermo Fisher). The samples were again washed with PBS 3 times with 1 h incubation between the washes. The washed samples were mounted in Vectashield mounting medium with DAPI (Vector laboratories) and cured overnight at 4°C before imaging. Imaging was conducted using a confocal laser scanning microscope (Leica STELLARIS 5) equipped with 5x/0.15, 10x/0.40 CS2 and 20x/0.75 CS2 air objectives, 405 nm, 488 nm, and 555 nm filter cubes controlled by LAS X imaging software; Leica).

3.1.6. Live/Dead staining

Thin vertical slices from the center of the device were cut using a razor blade and stained for 25 min at 37°C in a live/dead staining solution. The working dye solution contained 18.9 µg/mL propidium iodide (Fisher Scientific) and 1.1 µg/mL Calcein AM (Fisher Scientific) diluted in

culture medium. Images were captured using an IX81 Olympus Microscope with a FITC filter cube (Ex: 482/35; Em: 536/40) and a Texas Red filter cube (Ex: 525/40; Em: 585/40). Image processing was done using Fiji/ImageJ with grid/collection stitching plugin.

3.1.7. Dithizone staining

To prepare the dithizone staining solution, 5 mg of dithizone (Sigma) was dissolved in 1 mL of DMSO, followed by the addition of 4 mL of PBS and thorough mixing to dissolve as much as possible. The solution was then filtered using a 0.22-micron syringe filter and used within 24 h. For staining, at least 10 aggregates were incubated with 100 µL of the dithizone solution in a microcentrifuge tube for less than one minute. They were then rinsed repeatedly with PBS until the solution was completely clear. Finally, the aggregates were transferred to a 6-well plate containing 2 mL of PBS and were imaged using VWR® Trinocular Inverted Microscope under 40X magnification.

3.1.8. Histology

Fixed samples were processed at the Institut de recherche Clinique de Montréal (IRCM) for paraffin embedding, sectioning, deparaffinization, and staining. The 6 µm thick sections were cut orthogonal to the perfusion channel and stained with either Hematoxylin and Eosin or Masson's Trichrome. Imaging was conducted using a Zeiss Axio 200M automated inverted microscope with Zen Pro acquisition and analysis software.

3.1.9. Cell Culture

Mouse insulinoma cell line (MIN6) cells were cultured in high-glucose Dulbecco's Modified Eagle Medium (DMEM) supplemented with 10% FBS, L-glutamine, penicillin-

streptomycin (Invitrogen), and β-mercaptoethanol (Sigma). MIN6 cells were used between passages 25 and 40.

WA01H1 Human Embryonic stem cells (hESCs) obtained from WiCell and used under approval from Canada's Stem Cell Oversight Committee, were cultured and maintained on hESC-qualified Matrigel coated Sarstedt (red) plates in mTeSR medium (STEMCELL Technologies). The hESCs were passaged by washing in Ca^{2+} and Mg^{2+} free PBS and disassociated with TrypLE (Invitrogen) for single cell passaging or incubating for 4 min in 50 μM EDTA in PBS followed by obtaining cell clumps via cell scraper (Sarstedt) for colony passaging.

Human islets were obtained from Alberta Diabetes Institute Islet Core under a protocol approved both by the Alberta and McGill Institutional Review Boards. The obtained islets are cultured in 2% human serum albumin (HSA) substituted Connaught Medical Research Laboratories (CMRL) media for 24 h and were used for further experiments.

3.1.10. hESCs differentiation to pancreatic lineage

The hESCs were expanded in hESC-qualified Matrigel coated Sarsted (red) plates in mTeSR medium. Before confluency was reached, single cells were obtained and seeded on growth factor reduced Matrigel coated Sarsted (red) 6 well plates at a cell density of 1.35×10^6 cells in 2 mL mTeSR media supplemented with 10 μM Rho-Associated kinase inhibitor (STEMCELL Technologies) per well.

Pancreatic endocrine differentiation was performed following previously published protocols [15, 74] with modifications. The differentiation protocol involves a sequential addition of growth factors and small molecules across seven stages. The growth factors across different stages includes Activin A (Cat. 338-AC-50/CF), CHIR99021 (Cat. 4423/10), L-ascorbic acid (Cat.

A4544), Human Recomb. FGF7 (Cat. 78186.2), IWP-2 (Cat. 13951), ITS-X (Cat. 51500056), SANT-1 (Cat. 14933), retinoic acid (Cat. R2625-50MG), LDN193189 (Cat. SML0559), TPB (Cat. 565740), gamma secretase inhibitor XX (Cat. 565789-1MG), ALK5 inhibitor II (Cat. 14794) and T3- (3,3′,5-Triiodo-L-thyronine sodium salt) (Cat. T6397). The growth factors were obtained either from Cedarlane or STEMCELL technologies. Detailed medium formulations and growth factor compositions are provided in Table 3.1. Medium was changed daily during stages 1 to 6 and every other day during stage 7. On day 3 of stage 4 (S4), cells were detached using TrypLE and seeded into AggreWell400 plates (Stem Cell Technologies) at 1,000 cells per microwell in 5mL media per well. During stage 5, cells were maintained in AggreWells with careful handling to avoid dislodging aggregates, and 70% medium replacement. At the start of stage 6 (S6), aggregates were transferred to ultra-low attachment plates (Corning Cat. - CLS3471-24EA) and placed on an orbital shaker (CellTron Cat. 510925) at 100 rpm. For stage 7 (S7), aggregates were either cultured in suspension, encapsulated in alginate, or encapsulated within devices. These cultures were maintained for an additional 25 days with medium changes every other day.

Table 3.1: Differentiation media formulations

Stage	Basal Medium	Growth Factors
Stage-1	MCDB131 + 10mM glucose + 1.5 g/L NaHCO3 + 0.5% fatty acid free bovine serum albumin (FAF-BSA) + 1x GlutaMAX	+100 ng/mL Activin A +3 μM CHIR99021 (only day1)
Stage-2	MCDB131 + 10mM glucose + 1.5 g/L NaHCO3 + 0.5% fatty acid free bovine serum albumin (FAF-BSA) + 1x GlutaMAX	+0.25 mM ascorbic acid +50 ng/mL keratinocyte growth factor (KGF) + 1.25 μM IWP-2
Stage-3	MCDB131 + 10mM glucose + 2.5 g/L NaHCO3 + 2% FAF-BSA + 1x GlutaMAX	+0.25 mM ascorbic acid + 1:200 insulin-transferrin-selenium-ethanolamine (ITS-X) +50 ng/mL KGF + 0.25 μM SANT-1 + 1 μM retinoic acid + 100 nM LDN193189 + 200 nM TPB (PKC activator)
Stage-4	MCDB131 + 10mM glucose + 2.5 g/L NaHCO3 + 2% FAF-BSA + 1x GlutaMAX	+0.25 mM ascorbic acid + 1:200 ITS-X +2 ng/mL KGF + 0.25 μM SANT-1 + 0.1 μM retinoic acid + 200 nM LDN193189 + 100 nM TPB
Stage-5	MCDB131 + 20mM glucose + 1.5 g/L NaHCO3 + 2% FAF-BSA + 1x GlutaMAX + 1% Pen/Strep	+ 1:200 ITS-X + 10 μM zinc sulfate + 10 μg/mL heparin + 0.25 μM SANT-1 + 1 μM T3 + 100 nM Gamma secretase inhibitor XX + 10 μM ALK5 inhibitor II + 0.05 μM retinoic acid + 100 nM LDN193189
Stage-6	MCDB131 + 20mM glucose + 1.5 g/L NaHCO3 + 2% FAF-BSA + 1x GlutaMAX + 1% Pen/Strep	+ 1:200 ITS-X + 10 μM zinc sulfate + 10 μg/mL heparin + 1 μM T3 + 100 nM Gamma secretase inhibitor XX + 10 μM ALK5 inhibitor II + 100 nM LDN193189
Stage-7	MCDB131 + 20mM glucose + 1 g/L NaHCO3 + 2% FAF-BSA + 1x GlutaMAX + 1% Pen/Strep + 1x non-essential amino acids +1x Trace element A + 1x Trace element B	+ 1:200 ITS-X + 10 μM zinc sulfate + 10 μg/mL heparin + 1 μM T3 + 1mM N-acetyl cysteine

3.1.11. Device perfusion *in vitro* in custom bioreactor

To perfuse the human-scale device, a custom bioreactor was fabricated with milled polycarbonate (dimensions: 120mm*100mm*25mm; inlet and outlet ports of 5mm diameter; grooved pressure release ports of 10mm diameter). Devices were thoroughly cleaned by immersion in distilled water for 24 h in a 4-liter beaker. The 9-channel porcine scale devices were installed into the vascular bioreactor using autoclave resistant tie-wraps. The bioreactor was then assembled and connected to the perfusion tubing system. To ensure sterility, the bioreactor ports were loosened, and the entire setup was autoclaved using a humid vapor cycle for 30 min (Figure 3.1).

For studies involving rodent scale devices, a 5 cm long, 1 cm internal diameter temperature resistant clear silicone tubing (McMaster-Carr Cat. 5236K523) was utilized to house the device.

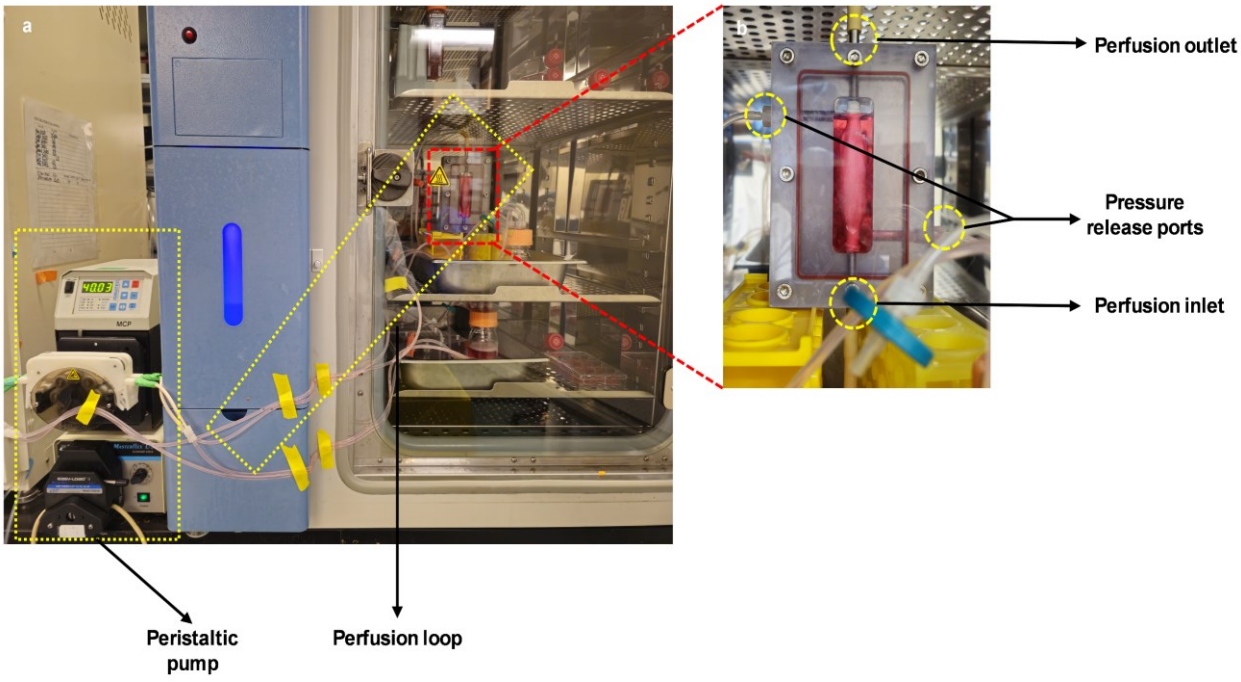

Figure 3.1: (a) *In vitro* perfusion setup connecting the bioreactor to the peristaltic pump; (b) device connected between the perfusion loop inside the bioreactor

The device was secured inside the tube with 1/16” straight connector (McMaster-Carr Cat. 5047K71) inserted in both ends of the device. Further the silicone tube was sealed using 1/2” tube connector (McMaster-Carr Cat. 5463K465) at both ends and this setup was connected between the perfusion loop connected to the peristaltic pump.

To immobilize MIN6 aggregates or SC-islets for *in vitro* studies, internal gelation of Protanal (FMC Biopolymer Cat. LF2040) 5% alginate was utilized. A 6% alginate solution was prepared by dissolving alginate powder in 4-(2-hydroxyethyl)-1-piperazineethanesulfonic acid (HEPES) buffer (10 mM HEPES, 170 mM NaCl, pH 7.4) and then mixed with 1M $CaCO_3$ (VWR) and 2.4M Glucono-δ-lactone (Sigma). The mixture was adjusted to achieve a suspension containing 5% alginate, 30 mM $CaCO_3$, and 0.6 mM Glucono-δ-lactone, with cell seeding densities of 10×10^6 cells/mL for MIN6 cells or 5000 to 7000 SC-islets per rodent scale device. After adding cells, the solution was carefully injected into the device using an 14G flexible ePTFE needle (McMaster-Carr, Cat. 75175A691). The device is gently tilted back and forth to ensure even distribution of the gel, followed by a 20-min gelation period before initiating perfusion. Perfusion was maintained using a peristaltic pump (Ismatech) placed inside the incubator set at 37°C with 5% CO_2. The culture medium flow rate was maintained at 40 mL/min for porcine scale devices and 25 mL/min for rodent scale devices except during insulin secretion experiments. Medium was manually replenished every two days under the biosafety cabinet to maintain sterile conditions.

For SC-islet encapsulation *in vivo*, aggregates were suspended in a 5% alginate hydrogel solution prepared from a 50:50 blend of ultrapure LVM and MVG alginates (Novamatrix). The solution was injected into the device with an 18G needle. To induce gelation, a concentrated calcium chloride solution (10 mM HEPES, 75 mM NaCl, 100 mM $CaCl_2$, pH 7.4) was perfused

through the system for 20 min. After gelation, the cell laden devices were kept in an autoclaved 500 mL bottle with S7 media.

3.1.12. Dynamic Glucose-stimulated insulin secretion (GSIS) assay

The tubing was flushed to clear the culture medium, and the devices were perfused in a single-pass flow configuration at a flow rate of 1.5 mL/min for 2 h using Krebs buffer supplemented with 2.8 mM glucose to eliminate residual glucose. The Krebs buffer consisted of 130 mM sodium chloride (Sigma), 4.7 mM potassium chloride (Sigma), 1.2 mM $MgSO_4$ (Sigma), 10 mM HEPES (Fisher), 2.5 mM $CaCl_2$ dihydrate (Sigma), 5.0 mM $NaHCO_3$ (Fisher), and 0.5% (w/v) bovine serum albumin (Sigma, A3294) dissolved in reverse osmosis water. The pH was adjusted to 7.4 using sodium hydroxide (Fisher).

The insulin secretion test was conducted by sequentially perfusing the device with Krebs solution under varying glucose concentrations. The protocol involved an initial 30-min perfusion with 2.8 mM glucose, followed by 45 min at 16.7 mM glucose, then a return to 2.8 mM glucose for 45 min, and finally 30 min with 20 mM potassium chloride. Samples were collected every 3 min, centrifuged immediately to remove potential cellular contaminants and stored at -20°C. For analysis, the samples were thawed and processed using an ELISA kit (ALPCO 80-INSMS-E01 or 80-CPTHU-E01.1) following the manufacturer's protocol. Absorbance measurements were recorded using a Benchmark Plus Microplate Spectrophotometer (Bio-Rad).

3.1.13. *in vivo* Pig experiments

All procedures adhered to ethical guidelines for animal care and use as approved by McGill University CMARC and CHUM's Research Ethics Committee (Protocol no. F2AE-115449). Non-

diabetic, immunocompetent pigs weighing approximately 35–50 kg were sourced from Ferme Triporc Inc.

Surgical Procedure:

To facilitate implantation, the devices were modified with a 'U-shaped' Polyurethane (PU) extension, allowing them to be implanted as an arteriovenous shunt between the right iliac artery and vein. For preparation of cell-free devices, the modified devices were loaded with alginate the day before surgery and incubated in HEPES buffer supplemented with 40 mM calcium chloride at 4°C. For preparation of cell-laden devices, SC-islets were mixed with alginate and loaded into the devices two h before surgery, then stored on ice in Stage 7 medium with 40 mM calcium chloride until implantation. During surgery, the iliac artery and vein were accessed, vascular clamps were inserted, and anastomosis was performed. The PU extension was connected to the vein and the device's end was sutured to the artery at a 45° angle using 6-0 polypropylene sutures, ensuring arterial inflow and venous outflow through the device. After removing the clamps, perfusion was confirmed by observing pulsation in the device. The incision was closed with #1 PDS sutures and the skin was sutured with 3-0 vicryl sutures

Pre/Post-Operative Care:

Pre- and post-operative care for the pigs included the administration of several medications to ensure their well-being and recovery. Antiplatelet therapy was provided with Clopidogrel (75 mg), while anticoagulation was achieved using Apixaban (0.5 mg/kg). To manage inflammation, Meloxicam (0.3 mg/kg) was administered, and Esomeprazole (40 mg) was given to prevent gastric ulcers. Throughout the study, the pigs were closely monitored for appetite, wound healing, and any signs of stress or lethargy until explant.

Device Retrieval and Processing:

Seven to eight days post-implantation, the pigs were euthanized, and the devices were carefully excised from the vasculature. Devices were perfused with HEPES buffer to remove residual blood, followed by perfusion with modified Bouin's fixative (3M formaldehyde, 0.9M glacial acetic acid). They were incubated overnight in the fixative. Samples from each device were paraffin-embedded and sectioned for subsequent staining.

3.1.14. Statistical/graphical analysis and graphical generations

Mean values and standard deviations were calculated and visualized using GraphPad Prism (version 9.5.0). Values were presented as mean ± SD. The displayed *in vitro* data were collected from 1 to 3 three biological replicates. *In vivo* validation was collected from 2 to 4 biological replicates. Some of the graphical illustrations were created using presets in BioRender.

3.2. Results

3.2.1. Fabrication of Vascular networks

Developing a macroencapsulation device with integrated vasculature that can be implanted as a vascular graft in the host's body required careful optimization of multiple critical parameters. For instance, the mechanical properties of the graft material such as compliance, tensile strength, and burst pressure must closely mimic those of native blood vessels. In addition, the graft surface must exhibit hemocompatibility to minimize the risks of thrombosis and premature occlusion. While achieving these properties, the vasculature must also ensure adequate porosity to facilitate convection-based mass transfer to the embedded cells within the device.

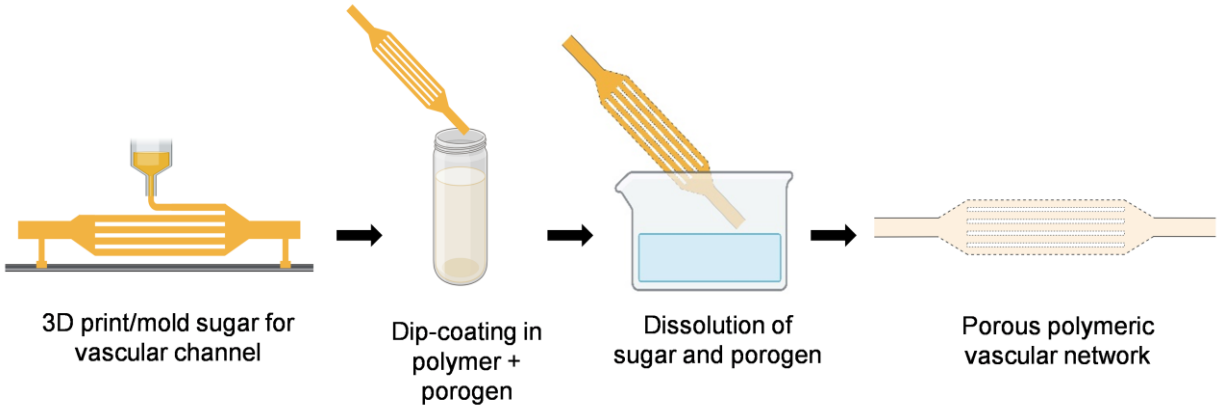

Figure 3.2: An An illustration of the vascular prosthesis fabrication process (created using biorender.com)

To fabricate the vascular network, we have developed a technology that utilizes sugar glass as sacrificial material to create vascular networks from simple to complex geometries. The carbohydrate glass templates are 3D printed or molded to the intended geometry followed by dip coating the sugar glass with a polymeric solution. After dip coating, the sacrificial glass is dissolved in water to produce a polymeric tubular vascular network (Figure 3.2.). For the graft material, we selected a commercially available PU (Chronoflex AR). PU is widely researched for

its application in vascular grafts, artificial heart and pacemakers due to its biocompatibility, durability, good tensile strength and non biodegradability [75, 76]. In addition, they are also soluble in commonly used organic solvents thus making them an ideal candidate for dip coating applications. To make the graft porous and create inter-connected pores throughout its wall thickness, we incorporated NaCl as porogen in the dip-coating solution.

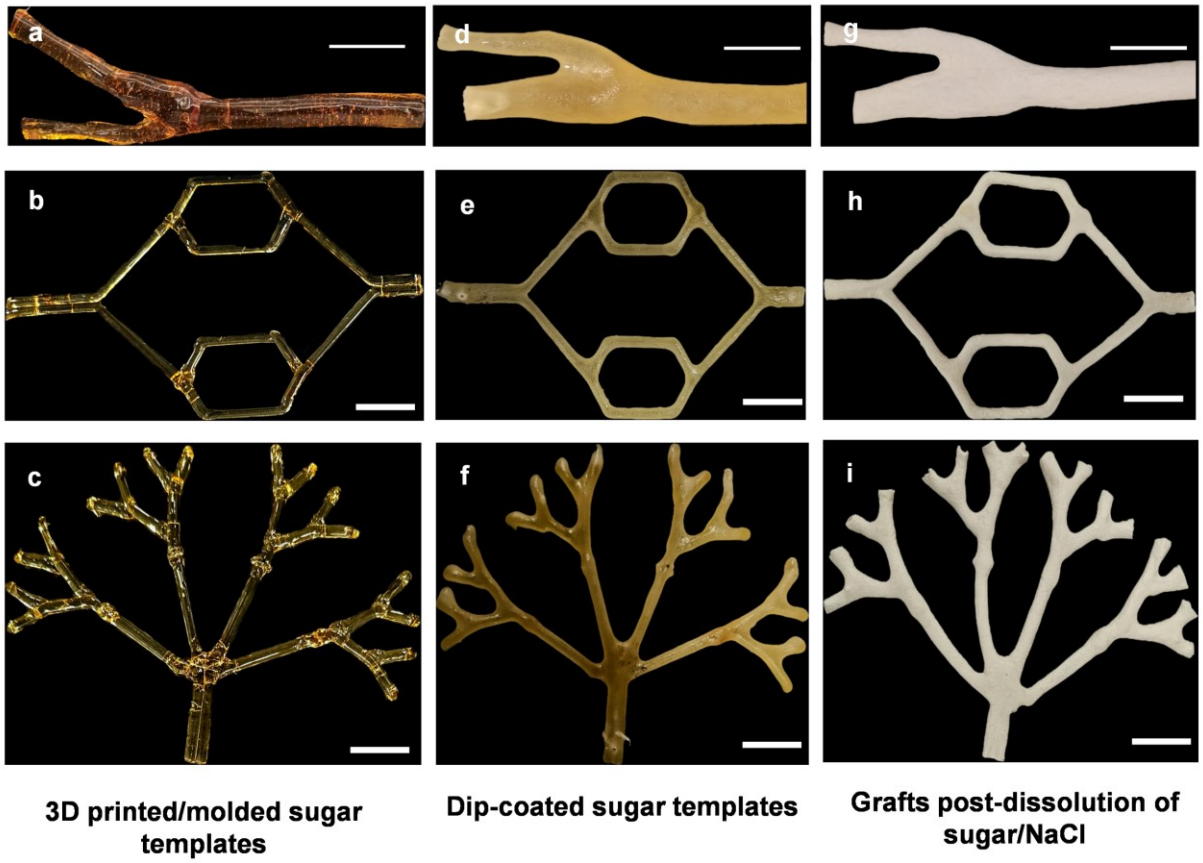

Figure 3.3: Representative images of fabricated vascular graft models; (a-c) 3D printed sugar lattices; (d-f) polymer coated sugar lattices' (g-i) polymeric vascular prosthesis post dissolution of sugar templates; scale bars – 2cm

Previous studies in our lab demonstrated that the porogen size and concentration had a significant effect on the porosity of the vascular graft and a porogen size > 45 µm and a NaCl-to-polymer weight ratio of 6:4 provided maximum porosity without compromising the mechanical

properties of the graft. The mechanical properties essential for a vascular graft such as burst pressure and longitudinal tensile strength of grafts using this dip-coating concoction were also studied and they were comparable to that of a commercially available vascular graft. Additionally, platelet adhesion studies confirmed that the grafts exhibited minimal thrombogenicity compared to commercially available Teflon grafts, further validating their hemocompatibility. Hence, we decided to move forward with this specific dip-coating mixture. With our sugar printing and dip-coating technology, we had successfully fabricated vascular networks with geometries ranging from simple bifurcation (Figure 3.3 g) commonly seen in carotid artery to complex multi-branched structures such as a looped duplicated fork and a triplicated fork with branching ends (Figure 3.3 h,i) mimicking renal arterial patterns. Hence this technology could pave way for fabricating a multitude of complex bioartificial organs.

3.2.2. Perfusable encapsulation device fabrication

After successfully synthesizing porous vascular networks, our next objective was to fabricate an encapsulation device with embedded vascular networks by creating a cell-loading compartment layered around the vascular channels. We employed a similar approach to the

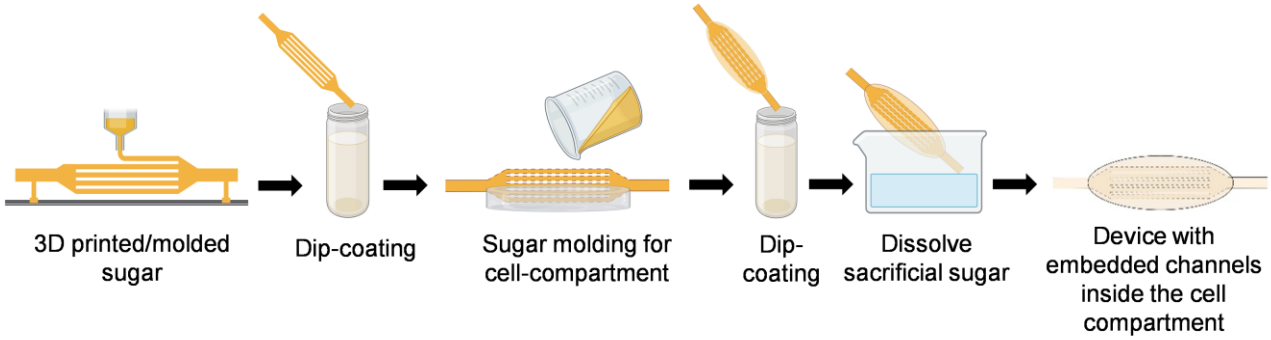

Figure 3.4: An illustration of the encapsulation device fabrication with embedded channels (created using biorender.com)

vascular network fabrication process, which involves iterative sugar molding and coating. Specifically, the vascular networks were created in a similar manner, but before dissolving the sacrificial template, an additional layer of sugar was molded over the previously coated sugar, followed by dip-coating the newly molded sugar layer (Figure 3.4).

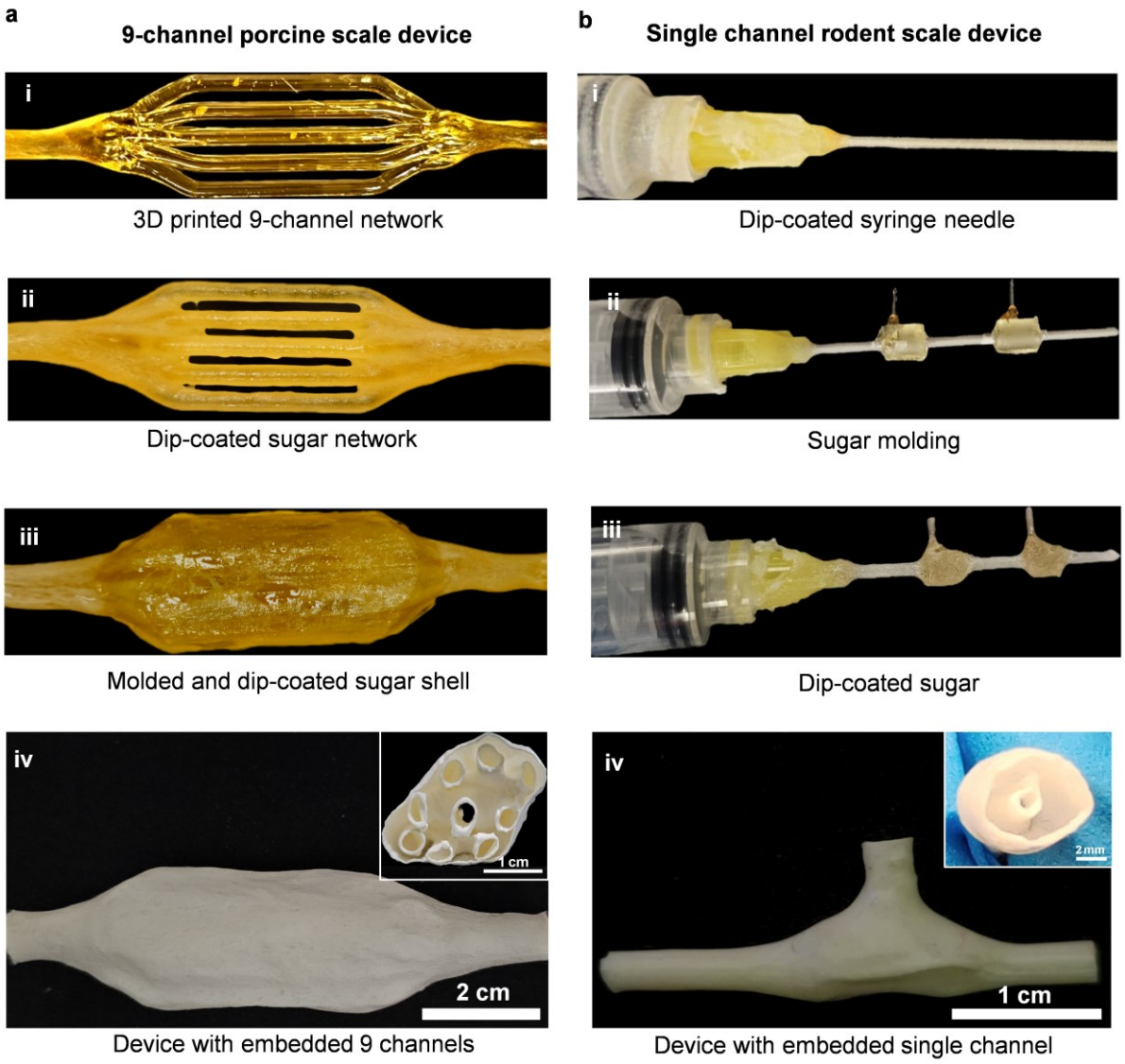

Figure 3.5: Representative images of device fabrication process, 9-channel porcine scale device (a i-iv) and single channel rodent scale device (b i-iv); cutouts in (iv) displays the respective cross-section of the devices.

A critical consideration during this process is ensuring minimal interaction between the dip-coating polymer and the sacrificial material, especially at elevated temperatures of approximately 175°C. Furthermore, the sacrificial material must resist degradation by the solvent used to dissolve the polymer. In this context, PU emerged as a suitable candidate, as it can withstand high temperatures and demonstrates minimal interaction with sugar glass in the presence of dimethylformamide (DMF). Another essential parameter to consider is the property of the dip-coated PU to swell upon hydration. Due to the high porosity of the graft, the prosthesis undergoes significant swelling after the sacrificial sugar template is dissolved. To enable effective coating of the second layer of molded sugar, the same dip-coating mixture was utilized to homogenize the swelling. Finally, a PU coating without porogen was applied to create an impermeable external layer, thereby preventing unintended external flows *in vitro* and reducing risks of hemorrhage post-transplant.

For this study, we developed two prototypes of the vascular lattice device tailored to the animal models intended for testing. For the porcine model, a nine-channel device approximately 6 cm in length with a cell-loading compartment volume of 12 mL was developed (Figure 3.5 a-iv). As a simpler prototype requiring a reduced therapeutic cell dosage, we also created a rodent-scale single-channel device measuring 2 cm in length with a cell loading compartment volume of 100–150 µl. To fabricate the vascular channels of the rodent-scale device, a 20-gauge blunt-tip syringe needle was used, followed by iterative sugar molding and coating (Figure 3.5 e-h).

3.2.3. Device characterization

Given that our vascular lattice device relies on convection-based mass transfer to the cells through perfusion within the channels, ensuring adequate porosity in the vascular channels was a key design objective. Porosity not only supports nutrient and oxygen diffusion but also facilitates

the removal of cellular waste, which is critical for maintaining cell viability and functionality in an *in vivo* setting. Drawing from previous studies conducted in the lab, we determined that a porogen size of >45 μm and a concentration of 60% by weight in the sugar dip-coating solution provided the optimal balance, achieving the highest porosity while preserving the necessary mechanical integrity of the graft.

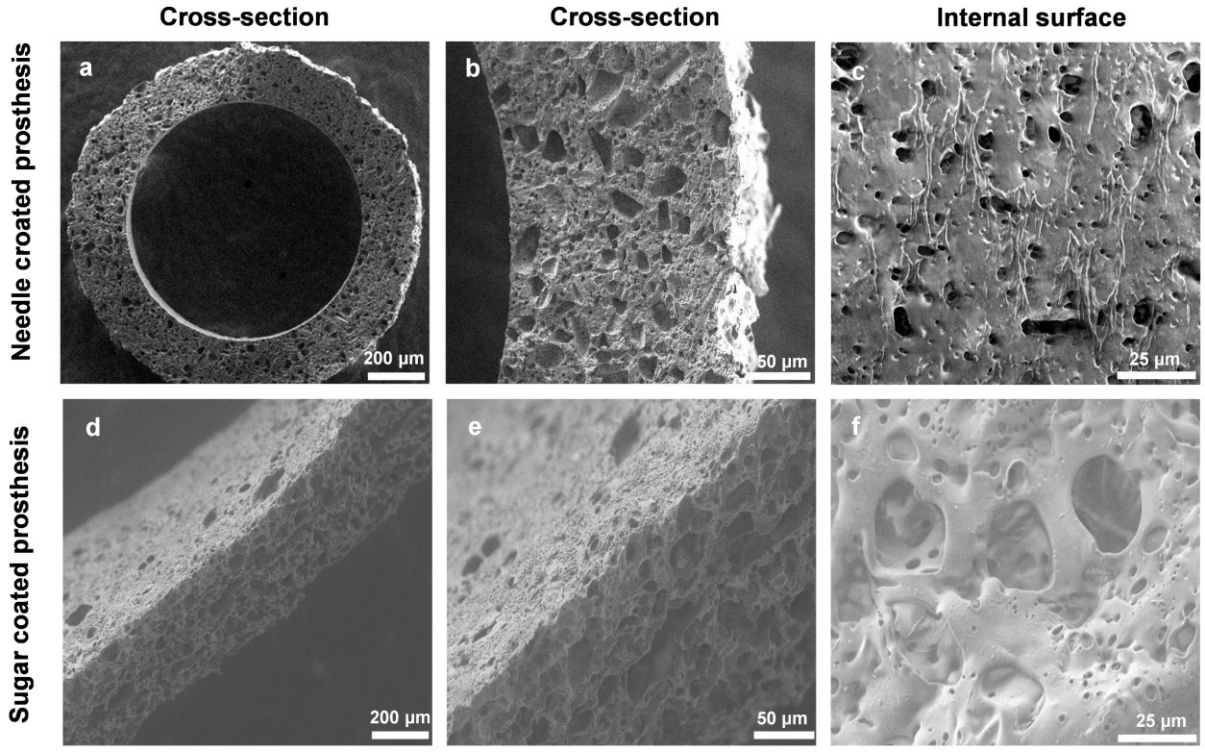

Figure 3.6: Scanning electron microscopy (SEM) images of (a-c) needle-coated vascular channel; (d-f) sugar-coated vascular channel and their respective cross sections and internal surface

The same polymer blend was used to dip-coat needles for the fabrication of rodent-scale devices to ensure consistency in the structural and functional properties between different device prototypes. To validate that the needle coating preserved porosity comparable to the sugar-coated prosthesis, SEM was performed on the needle-coated prosthesis to examine its microporous structure. The SEM images confirmed the retention of the porous network throughout the graft,

indicating that the process successfully retained the porosity to the needle coating (Figure 3.6 a-c). Additionally, SEM analysis revealed an improvement in the internal surface smoothness of the needle-coated prosthesis compared to the sugar-coated counterpart based on qualitative observation. This improvement in luminal smoothness could reduce the likelihood of platelet adhesion and subsequent thrombosis, a critical factor for maintaining long-term patency *in vivo [77]*.

3.2.4. Device validation *in vitro*

We have successfully developed vascular lattice device prototypes incorporating a cell compartment and perfusable vascular channels seamlessly embedded within them. The cell compartment is specifically designed to accommodate the loading of metabolically active cells, while the vascular channels can be irrigated to facilitate the efficient exchange of nutrients, oxygen, and metabolic waste. To replicate *in vivo* fluid flow conditions within the cell-laden devices, we designed and fabricated a custom bioreactor system. This bioreactor allows the encapsulation device to be integrated into a perfusion loop driven by a peristaltic pump. A key feature of this bioreactor system is its capability for aseptic loading of cells within the device inside a biosafety cabinet, ensuring sterility during the cell-loading process. Following the loading step, the entire setup can be safely transferred to a CO_2 incubator, which provides optimal temperature, humidity, and gas exchange conditions for maintaining cell viability and functionality over extended culture periods. Once inside the incubator, the vascular channels can be perfused using the peristaltic pump located outside the incubator and this setup offers precise control on flow rates. Additionally, the modular design of the bioreactor permits easy disassembly and reassembly, simplifying maintenance and reducing the risk of contamination during repeated experiments.

Given that our device offers the flexibility to load cells embedded in a variety of matrices, it can be tailored to promote vascularization or provide immunoprotection, depending on the application. For this study, we specifically chose to embed the cells in an immunoprotective biopolymer, using high-concentration alginate as the matrix. Alginate, an anionic polysaccharide, forms a hydrogel upon interaction with cationic ions and is well-suited for cell encapsulation due to its cytocompatibility and minimal immunogenicity [78]. This material has been widely used in various settings, including achieving normoglycemia through allografts in both immunocompetent mice [78] and non-human primates [79]. After gelation, the alginate acts as a permselective barrier against immune antibodies [80], while the device's internal vascular network and external casing serve as nutrient sources and structural support, respectively.

3.2.4.1. MIN6 survival in rodent scale devices

To validate the device's ability to support cell survival and function, we encapsulated MIN6 cells, an insulin-secreting and glucose-responsive pancreatic β-cell line derived from a mouse insulinoma tumor. The cells were encapsulated within the device using an alginate external gelation process with a final alginate concentration of 5% (w/v). Rodent-scale devices were loaded with MIN6 cells suspended in the alginate solution. Gelation was initiated using a gelling solution of 100 mM calcium chloride mediated external gelation ensuring the formation of a stable hydrogel matrix. Following loading and gelation, the bioreactor setup was transferred to a CO_2 incubator, where the system was perfused with DMEM supplemented with fetal bovine serum (FBS) at a flow rate of 25 mL/min for 48 h. At the end of the perfusion period, the alginate containing the embedded cells was isolated, and cross-sectional samples were obtained. Viability staining confirmed that the cells remained viable throughout the entire cross-section of the hydrogel under perfusion and similar results were observed in two biological replicates (Figure 3.7). The observed

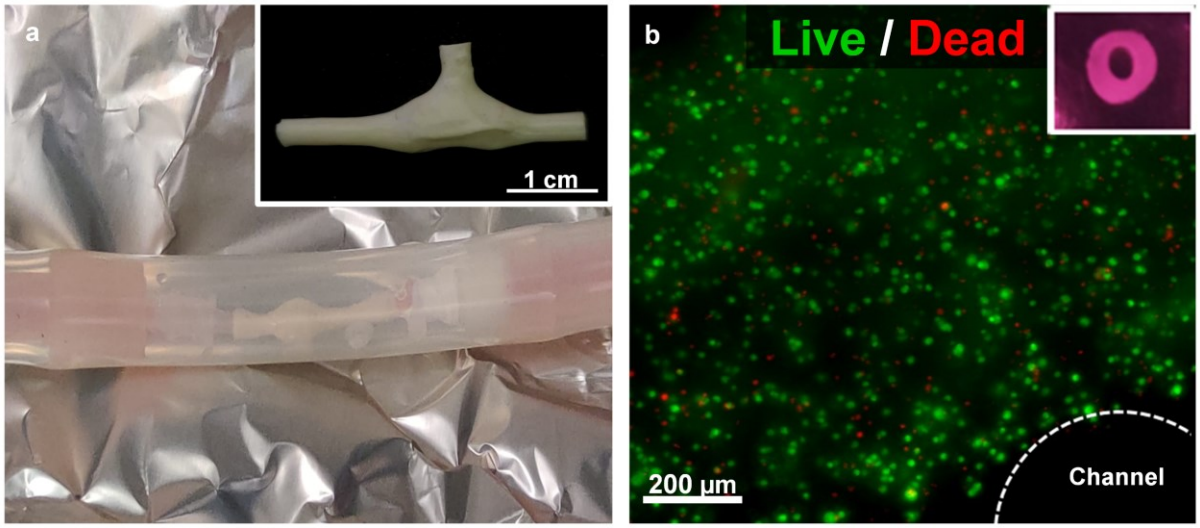

Figure 3.7: (a) in vitro perfusion of rodent scale device in a makeshift bioreactor; (b) Live/Dead (Calcein/PI) imaging of MIN6 (10^8 cells/mL) embedded in alginate within the rodent scale device post 48hr perfusion (25mL/min), insert showing the cross-section of the cell laden alginate obtained from the device.

viability of MIN6 cells across the entire hydrogel cross-section at 25 mL/min perfusion aligns with reaction-diffusion-convection models. Previous study in our lab reported a 0.98 mm viability radius at 4 mL/min. This was done using the equation of radial oxygen transport model $\mathbf{D_{eff}\nabla^2 CO_2 - R = 0}$; equation for effective diffusivity $\mathbf{D_{eff} = XD_{cells} + (1-X)D_{alg}}$; oxygen consumption rate $\mathbf{R = (RO_2 * C^2O_2/(Ks + C^2O_2))\ (1 - \delta(CO_2 - C_{cr}))X}$ and substituting the values of constants and scaling factor for convective transport and oxygen diffusion. [81]. Using this data, the theoretical viability radius at 25 mL/min is estimated to be 1.81 mm, which closely matches our experimental observation where the entire ~2 mm radius gel remained viable.

3.2.4.2. SC-islet survival and glucose response in rodent scale devices

SC-islets are a promising source of insulin-producing cells for cell therapy due to their superior availability compared to cadaveric donor islets. Following established protocols from previous studies [15, 74], we successfully generated pancreatic progenitors with >60%

PDX1^{+}/NKX6.1^{+} cells which were subsequently aggregated and further differentiated into mature S7 pancreatic SC-islets in suspension culture.

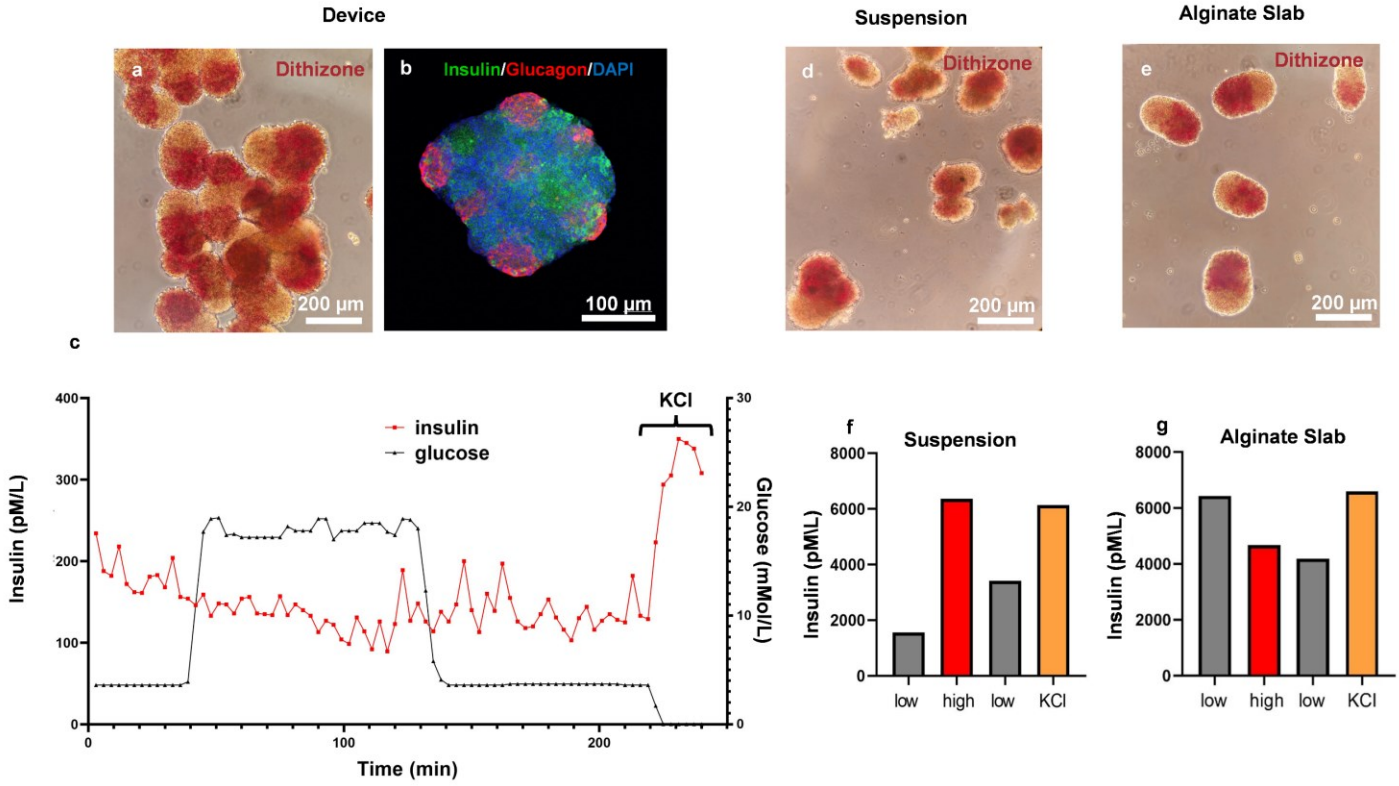

Figure 3.8: (a,d,e) Dithizone stained images of S7 SC-islets cultured in Device, suspension and Alginate slab respectively; (b) Laser confocal microscopic image of device cultured S7 SC-islets immunostained for maturation markers Insulin/Glucagon (Green/Red) and DAPI (Blue); (c,f,g) Insulin response graphs of S7 SC-islets cultured in Device, suspension and Alginate slab respectively.

Looking at the dithizone-stained images (Figure 3.8 a,d,e), the suspension-cultured S7 aggregates exhibit a higher degree of cell detachment and increased dead cell debris, whereas the device-encapsulated group and the alginate slab control group maintain high insulin content with minimal cell detachment at the aggregate surface. This suggests that alginate encapsulation has provided a more cytofriendly microenvironment, promoting the viability of S7 aggregates, which in turn led to a higher population of insulin-laden aggregates.

Examining the GSIS graph (Figure 3.8 c), it is evident that insulin secreted by the encapsulated cells successfully diffused through the alginate matrix, entered the perfusion channel, and reached the outflow. This confirms that the device retained its functionality, and in an *in vivo* setting, insulin would likely be delivered into the bloodstream when implanted as a vascular graft. However, analysis of the Insulin-Glucose vs. Time plot reveals that insulin levels remained at a basal concentration of approximately 200 pM/L, and instead of rising in response to glucose stimulation, they initially declined as the assay progressed. A noticeable peak at 110 min, reaching 200 pM/L by the end of the glucose stimulation phase, did not reflect a robust GSIS response. In contrast, KCl stimulation elicited a stronger insulin response, with levels increasing to approximately 350 pM/L, indicating that the SC-islets were still capable of insulin secretion after 48h of device perfusion.

The suboptimal GSIS response can be due to several factors – including insufficient removal of glucose from the culture media remaining within the gel, or a detrimental impact on SC-islets during the 48 h of immobilized culture thus affecting proper glucose sensing. However, KCl stimulation elicited a better response as KCl bypasses the glucose-sensing pathway, directly depolarizing voltage-gated potassium channels, thereby triggering rapid insulin secretion independent of glucose metabolism. Similar trends were observed in the alginate slab control groups, in contrast, non-encapsulated suspension-cultured β-cells responded well to both glucose and KCl stimulation. This discripancy in GSIS could also be attributed to the charge properties of the alginate matrix that might have influenced insulin diffusion. Calcium crosslinked alginate is negatively charged, while insulin, at physiological pH, carries a slight positive charge [82]. This charge interaction could have led to intermittent insulin accumulation within the encapsulation matrix, causing delayed or pulsatile insulin release. Furthermore, the delayed and attenuated

insulin response may also be attributed to the intrinsically lower glucose sensitivity of stem cell-derived islets (SC-islets) compared to native pancreatic islets [15].

Despite these challenges, microscopic analysis confirmed that device-encapsulated β-cells exhibited robust insulin content and minimal cell detachment, while also expressing key maturation markers. These results suggests that the SC-islets remained viable under continuous perfusion for 48 h, which is a significant milestone toward preclinical studies.

3.2.4.3. Human islets survival and glucose response in rodent scale devices

Even though pancreatic beta cell differentiation protocols have seen significant advancements in recent years, they still fall short of achieving the same level of glucose sensing and insulin secretion control as primary human islets, [19, 74] Human islets exhibit superior functionality, characterized by precise GSIS and high insulin storage capacity, enabling rapid and sustained responses to fluctuating glucose levels and this is further enhanced by the native paracrine interactions between beta, alpha, and delta cells population in an endogenous islet.

Given the inherent modularity of our device and its capacity to accommodate a diverse array of cell-matrix combinations tailored to specific applications, it offers significant potential to enhance existing donor islet transplantation strategies. To assess the device's performance to sustain endogenous islets, we encapsulated primary human islets derived from deceased donors and evaluated their viability and functionality under perfusion conditions.

The GSIS results showed that he device-encapsulated islets demonstrated a functional response to glucose and KCl stimuli, although the glucose response peaks exhibited some degree of variability. The suspension control group responded to GSIS as expected, with clear and consistent peaks, while the alginate slab-encapsulated islets showed only a small increase in insulin

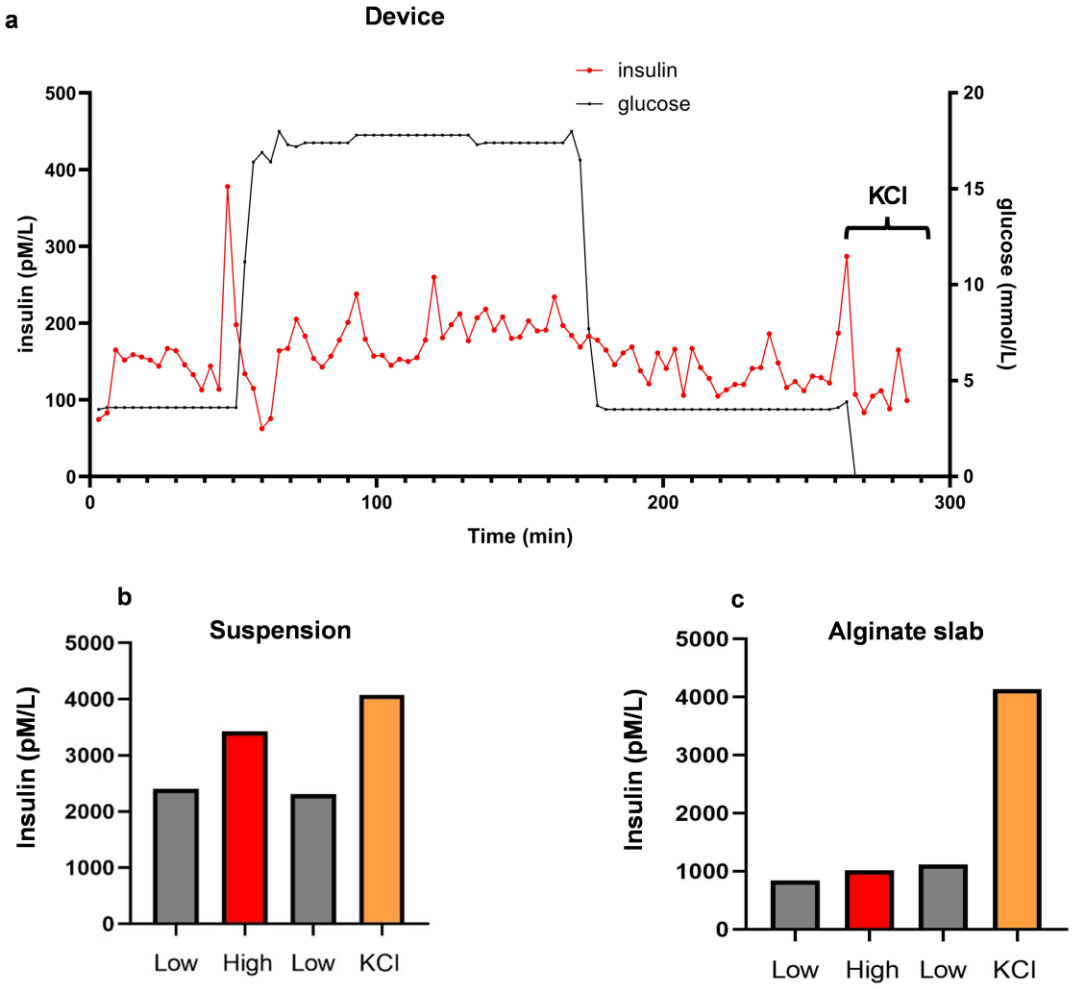

Figure 3.9: (a) Insulin response graphs of Human islets cultured in Device under perfusion; 5000-7000 islets per device, (b) suspension and (c) alginate slab

upon glucose stimulation but a strong response to KCl (Figure 3.9). Although these experiments were only conducted with one islet donor, the limited glucose responsiveness observed both with SC-islets and adult human islets suggests that this observation is not associated with a lack of cell maturation, but rather with intrinsic factors created by the hydrogel. Again, given the rapid insulin response to KCl, the main hypotheses lie with either insufficient glucose washout or detrimental effects of the high-concentration gel on SC-islet and islet health (oxygenation, mechanical stimuli,

biochemical stimuli). Future experiments should investigate whether islets recovered from the gels, with GSIS applied thereafter, show glucose responsiveness to delineate these hypotheses.

Overall, this pilot experiment with endogenous human islets is promising. The vascular lattice device demonstrated functional insulin secretion in response to both glucose and KCl stimulation yet further Live/Dead analysis is required to confirm that the entire islet population survived the perfusion. Although fluctuations in insulin secretion were observed, they are likely attributable to encapsulation limitation, or charge-related insulin retention within the encapsulation material. These findings indicate that the vascular lattice device holds strong potential as a platform for islet transplantation.

3.2.4.4. MIN6 survival and glucose response in single vs multichannel porcine scale devices

To evaluate the mass transfer efficiency of a multi-channel design compared to a single-channel design, we encapsulated MIN6 cells in a 9-channel porcine-scale device and a single-channel device of similar dimensions. The encapsulation was done with 5% working concentration of alginate solution with an internal gelation system comprising calcium carbonate and glucono-δ-lactone (GDL) to initiate gelation. Following loading and gelation, the devices were perfused with DMEM at a constant flow rate of 40 mL/min for 48 h. At the end of the perfusion period, we dynamic GSIS assay to assess cell functionality. Subsequent viability staining of cross-sectional samples from each device revealed that the 9-channel devices supported a higher population of viable cells around the perfusion channels compared to the single-channel devices, where the viable cell population was significantly lower (Figure-3.9 b,d). Furthermore, the GSIS assay demonstrated that cells in the 9-channel devices exhibited response to glucose, while cells in the single-channel devices showed diminished functional response under the same conditions (Figure 3.10 c,e).

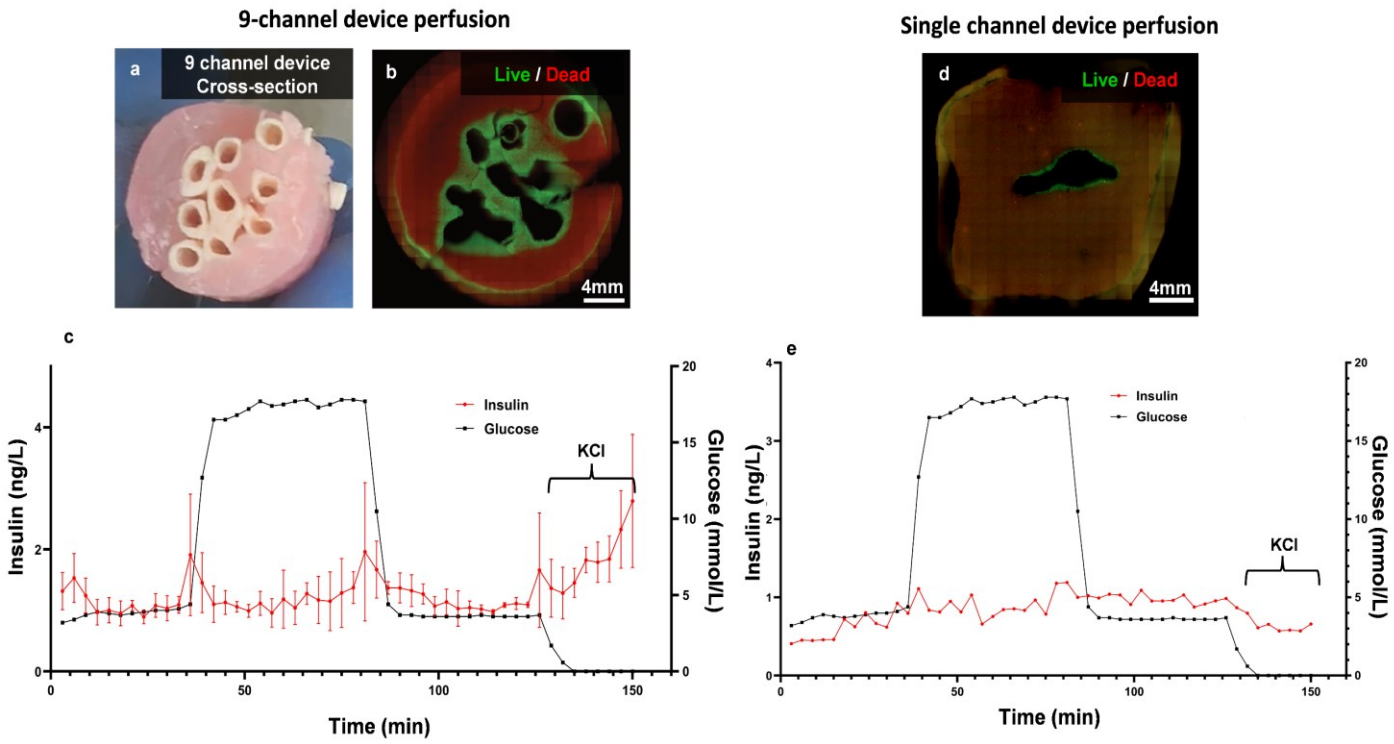

Figure 3.10: (a,b,c) Cross-section of the 9 channel device with MIN6 (10^8 cells/mL) embedded alginate, the respective Live/Dead (Calcein/PI) stained image and insulin response curve; (d,e) Live/Dead (Calcein/PI) stained image of single channel device with MIN6 (10^8 cells/mL) embedded alginate and the respective insulin response curve.

The primary objective of this experiment was to evaluate the impact of perfusion channel number and configuration on the viability and function of encapsulated cells in a scaled-up device designed to deliver a therapeutically relevant dosage for human patients. In scaled-up devices, the single-channel configuration exhibited reduced cell viability, likely due to inadequate nutrient and oxygen distribution (Figure 3.10 d). In contrast, the 9-channel device demonstrated a substantial improvement in cell viability profile with increased viable cells around the 9 channels (Figure 3.10 b). The GSIS profile of the 9-channel device revealed distinct insulin peaks at the start and end of glucose stimulation, reaching up to 2 ng/mL, with a stable basal level of approximately 1 ng/mL Looking at the KCl response, there is a gradual increase in insulin level instead of an instantaneous

increase after KCl stimulation. This suggests that there is a diffusion limitation at a larger scale even with 9 channel configuration. In comparison, the single-channel device failed to generate a significant GSIS response, with insulin levels remaining at or below 1 ng/mL throughout the assay (Figure 3.10 c,e). This discrepancy suggests that a single channel was insufficient for delivering the required nutrients and oxygen in human scale devices, leading to cell death and loos of function. Additionally, the internal gelation process used for alginate polymerization may have led to acid accumulation in single channel devices affecting cell viability whereas the acids would've been readily removed in multichannel devices during perfusion due to increased surface are for diffusion. These findings strongly indicate that a multichannel perfusion interface is essential for human-scale devices to sustain viable islet population and preserve functional insulin secretion.

3.2.5. Device validation *in vivo*

After evaluating cell survival and function *in vitro*, we proceeded to *in vivo* validation to assess whether our devices could maintain patency and functionality under blood perfusion without graft occlusion. Porcine models were selected due to their vascular anatomy closely resembling that of young human adults. To facilitate implantation, the single-channel porcine-scale devices were redesigned with a 'U'-shaped extension (Figure 3.11 a,b) to enable their use as arteriovenous shunts between the abdominal iliac artery and vein. This shunt approach was chosen over interposition or bypass techniques to ensure animal survival during the study even in the event of device occlusion.

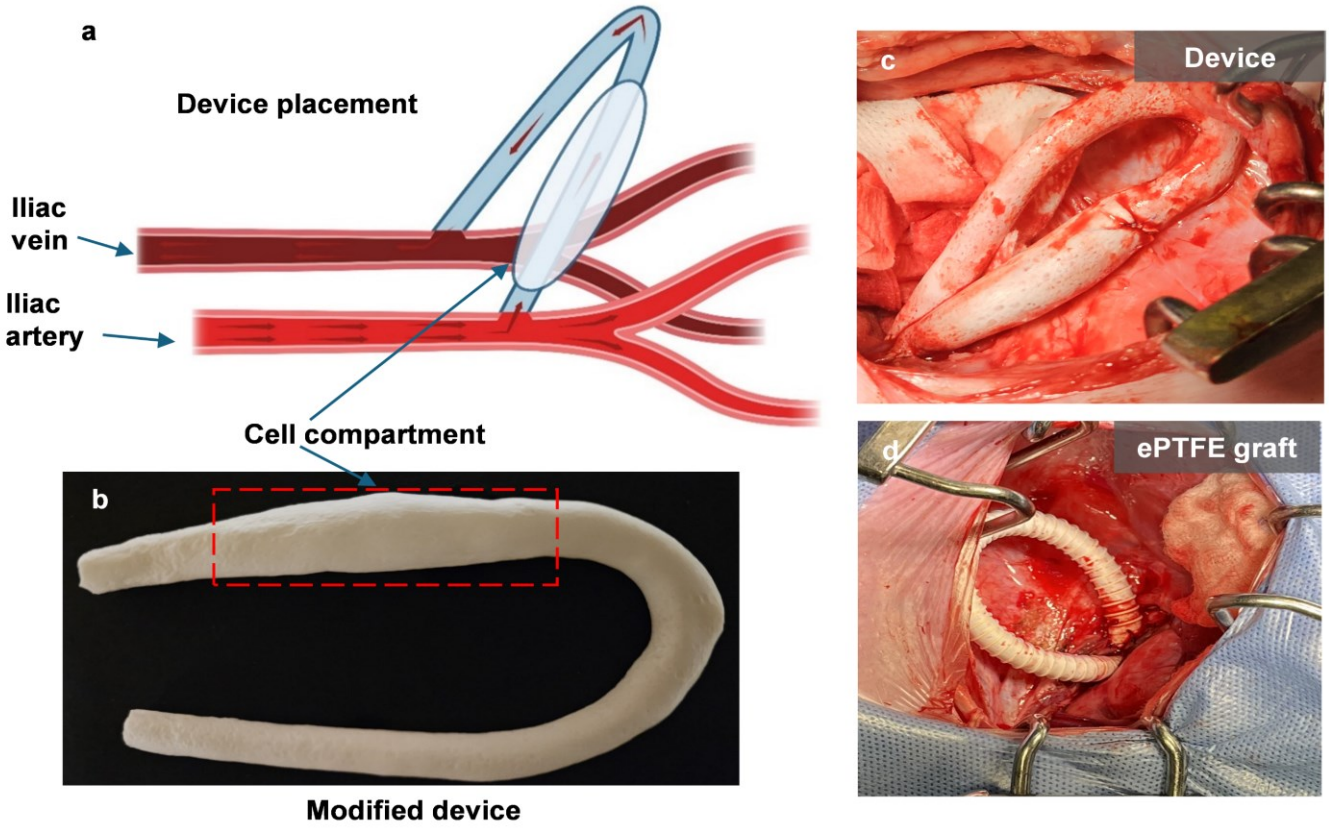

Figure 3.11: (a) Illustration of the intended device placement in porcine models (created using biorender.com); (b) Modified single channel porcine scale device; (c,d) representative images of Device and ePTFE control graft after implantation.

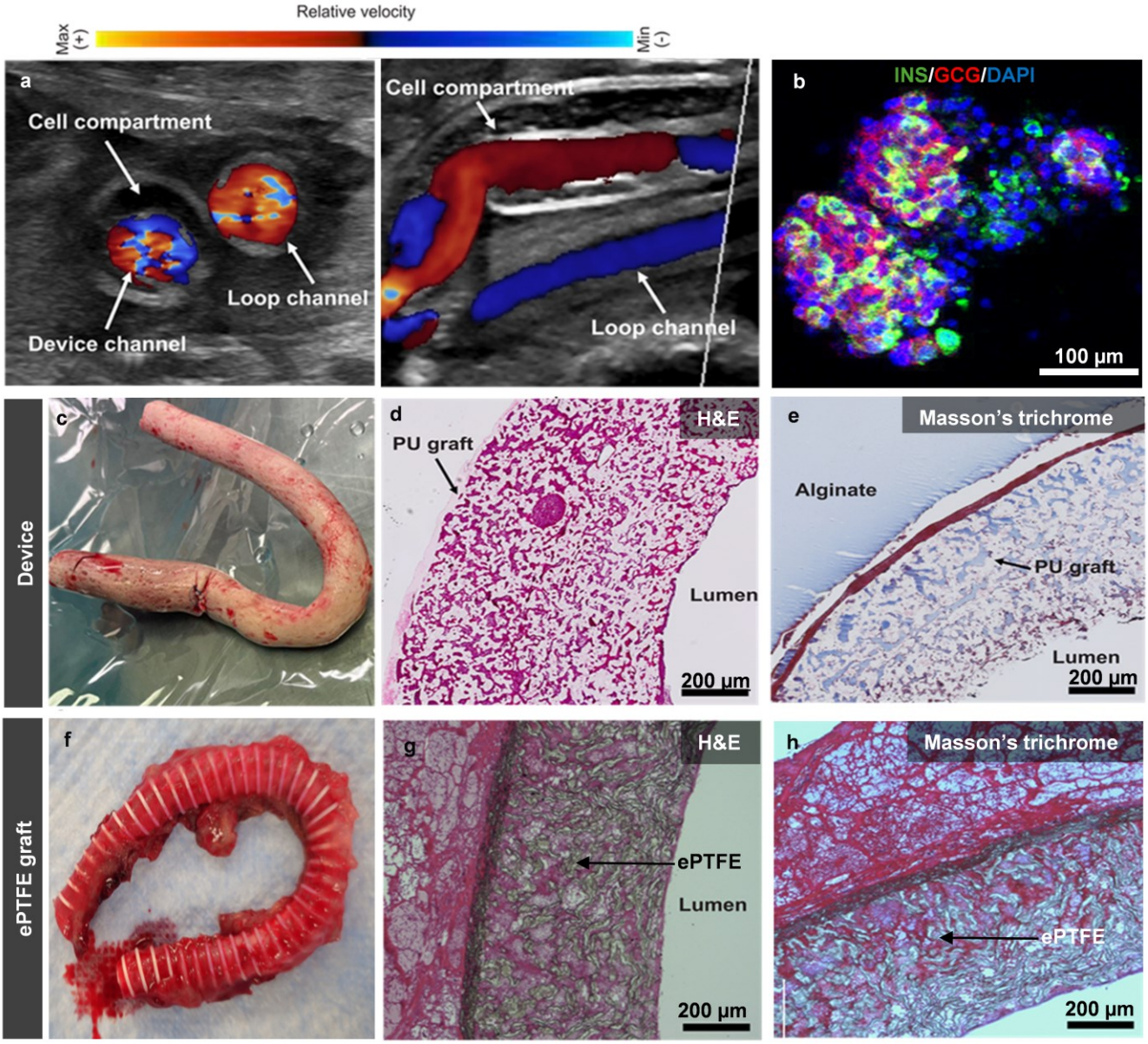

Figure 3.12: (a) Doppler ultrasound image of blood flow in the device before explanation; (b) Laser confocal microscopic image of in vivo device cultured S7 SC-islets immunostained for maturation markers Insulin/Glucagon (Green/Red) and DAPI (Blue); (c,f) representative images of device and ePTFE control graft post explant respectively; (c,f) H&E stained images of device and control graft sections respectively; (e,h) Massion's trichrome stained images of device and control graft sections respectively.

Four devices were implanted in four individual pigs, two cell-free devices containing alginate in the cell compartment and two devices loaded with Stage-7 SC-islets encapsulated in alginate. To maximize immunoprotection, we selected a 50:50 mixture of Pronova LVM:MVG

alginate from Novamatrix at a 5% concentration to embed the cells. This specific alginate mixture is expected to exclude antibodies in approximately 80% of the gelled alginate volume [80]. As a control, a commercial ePTFE vascular graft was implanted in one pig following the same surgical procedure.

The Doppler ultrasound images confirm continuous blood flow throughout the vascular lattice device, with an average flow rate of 800 mL/min. Given that typical arteriovenous grafts receive 600–2000 mL/min [83], this suggests that the device remained patent throughout the 7-day *in vivo* perfusion period. Importantly, the surgical procedure was successful, as all pigs survived without complications, further validating the device's biocompatibility and stability in a physiological environment. Upon closer examination, the blood flow within the device channel appeared turbulent, with significant backflow, as indicated by the red and blue gradients in the Doppler images, which reflect the flow direction relative to the probe (Figure 3.12 a). In an ideal scenario, a uniform flow is expected in an arteriovenous shunt. The observed turbulence and retrograde flow may be attributed to a slight kink in the device, which became evident after excision (Figure 3.12 c). This distortion in the structure could have disrupted the expected flow pattern, potentially affecting perfusion efficiency. Despite this, the exterior of the device exhibited minimal tissue attachment, indicating a low fibrotic response, which is a positive sign for long-term biocompatibility. Histological analysis further supports the patency and functionality of the device. H&E staining revealed a clear lumen without any signs of thrombus formation, reinforcing that the device successfully prevented occlusion during perfusion (Figure 3.12 e). Masson's trichrome staining also demonstrated a clear lumen but revealed a 20 μm thick layer of collagen deposition between the exterior of the lumen and the alginate matrix (Figure 3.12 f). While collagen deposition is often associated with the early stages of endothelialization and tissue

integration in vascular grafts, its presence at the interface of the micropores may obstruct mass transfer, potentially hindering glucose and insulin diffusion. SC-islets within the device remained viable throughout the 7-day perfusion period, expressing key maturation markers such as insulin and glucagon, confirming their sustained viability which is a significant milestone (Figure 3.12 b).

These findings reinforce the potential of the vascular lattice device as a viable platform for islet transplantation. However, further long-term implantation studies are necessary to investigate how prolonged perfusion affects collagen deposition and micropores blockage, which could impact nutrient exchange and insulin diffusion.

4. Chapter 4

4.1. Discussion

Cell encapsulation is a promising approach for treating T1D by enabling the transplantation of insulin-producing cells without requiring lifelong immunosuppression. This is especially crucial due to the autoimmune dysregulation in T1D, where the host immune system attacks the pancreatic beta cells, resulting in insulin deficiency and hyperglycemia. Although transplanting donor islets serves as a temporary solution to treat T1D, the allograft also faces the same fate of immune mediated destruction [84]. By incorporating the cells inside a permselective matrix, it physically protects the transplants from the immune system, aiding graft survival and functionality.

Several encapsulation devices have been developed to address the challenges of T1D treatment [85]. Among these, macroencapsulation devices such as DIABECELL®, Sernova's Cell Pouch System™, and ViaCyte's PEC systems etc. have gained significant attention. DIABECELL®, developed by Diatranz Otsuka Ltd., uses islets derived from pathogen-free neonatal pigs encapsulated in an alginate core surrounded by a poly-L-ornithine membrane. This device has shown promise in reducing hypoglycemic episodes and insulin dependence in clinical trials [86]. ViaCyte's PEC-Encap™ combines a semi-permeable encapsulation device with stem cell-derived pancreatic endoderm cells which mature into functional beta cells post-implantation [37]. Similarly, their PEC-direct® system, allow vascular ingrowth, but they require immunosuppression to prevent graft rejection, potentially compromising the immunoprotection aspect of encapsulation technologies [38]. TheraCyte's semi-permeable encapsulation device demonstrated some success but faces challenges with long-term functionality due to immune response and fibrosis [36]. Sernova's Cell Pouch System™ introduces a pre-vascularization step

through temporary implantation, which creates a supportive microenvironment before reloading with insulin-producing cells [87].

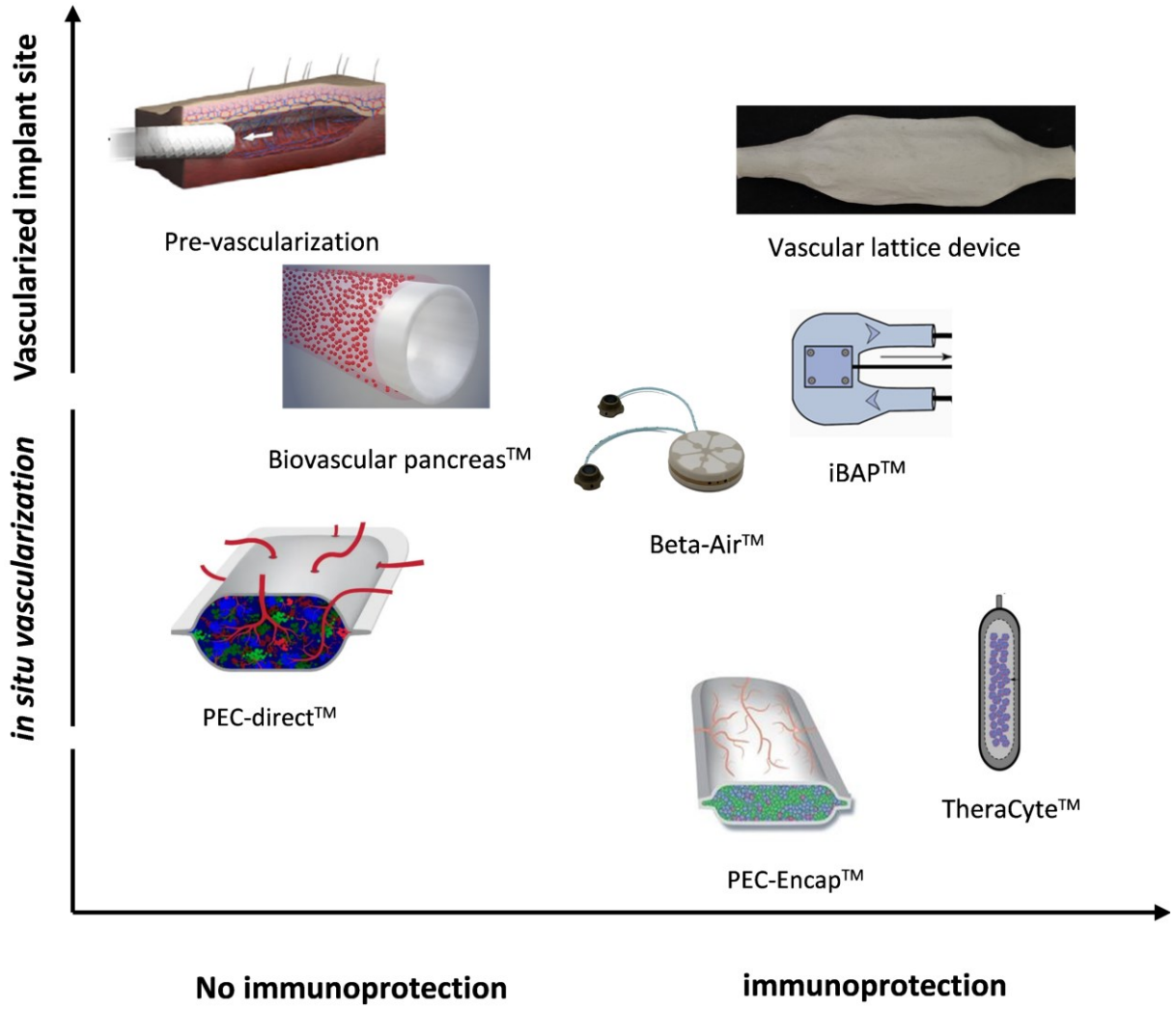

Figure 4.1: Immunoprotection and Vascularization Profiles of Notable Islet Encapsulation Devices

Although these devices have reached clinical trials, many fail to provide consistent long-term immunoprotection or early vascularization. The initial transplantation phase is particularly vulnerable, as the lack of oxygen and nutrients can result in the loss of up to 50% of transplanted cells, necessitating higher cell doses or periodic cell replenishment to achieve therapeutic efficacy.

Subcutaneous implantation sites, commonly opted for encapsulation devices, further enhance this issue due to inherently low oxygen availability at the site. Additional complications arise from fibrosis and immune responses at the device-tissue interface, which impair both function and longevity [88]. To address oxygenation and immunoprotection challenges, some designs incorporate complex features, such as Beta-O2's integration of an external oxygen supply system [40] and the intravascular bioartificial pancreas device (iBAP) incorporates a silicon nanoporous membrane to immunoisolate and support islet survival [63]. Further, a convection enhanced macroencapsulation device (ceMED) has also been demonstrated that incorporates proprietary ePTFE chambers for housing islets and a semi-permeable chamber to filter nutrients with an *ex vivo* perfusion setup while preventing entry of immune cells. [62]. Although these devices exhibited promising islet survival for a short term *in vivo*, the added device complexity compromises the long-term practicality similar to conventional insulin pumps and further, they often lead to material fatigue, fibrosis, thrombosis and foreign body responses ultimately diminishing device efficacy. Hence, developing a device that balances immunoprotection, vascularization, avoiding material interfaces and complex setups post transplantation is critical for achieving a close to ideal encapsulation device.

This project aimed to overcome these limitations by developing a uni-material convection-enhanced macroencapsulation device with embedded vascular channels. Unlike traditional approaches that depend on *in situ* vascularization, our design focuses on achieving efficient nutrient and oxygen delivery through convective flow with the flexibility of providing immunoprotection. By incorporating pre-formed vascular structures, the device addresses delayed vascularization and hypoxia, ensuring graft viability and functionality through immediate perfusion. The device is fabricated using an iterative process of sacrificial material 3D

printing/molding and polymer coating, resulting in a seamless encapsulation device with perfusable channels. Constructed entirely from PU, the device minimizes thrombosis and fibrosis risks while maintaining mechanical properties comparable to commercial vascular grafts.

In vitro validation and computational diffusion models from previous studies demonstrated that the device's performance depends on factors such as channel configuration, flow rates, cell density, and the diffusion properties of the encapsulation matrix. For instance, rodent-scale devices containing MIN6 cells showed significant cell survival under perfusion, whereas larger-scale devices emphasized the importance of multichannel interfaces. The increased surface area for mass transport in multichannel designs likely enhanced both cell survival and insulin responsiveness compared to single-channel devices of similar dimensions. Moreover, the internal gelation method used to polymerize alginate may have led to acid accumulation, potentially compromising cell viability due to the prolonged resident time of acid in single-channel designs. To ensure complete gelation, relatively long incubation in static conditions were applied prior to transplantation, which could be reduced through increased numbers of channels to reduce Ca^{2+} diffusion distances.

SC-islet survival studies in rodent-scale devices confirmed robust insulin content and minimal cell detachment, indicating viability under 48-hour perfusion. However, the GSIS profile did not exhibit distinct insulin peaks in response to glucose stimulation, while KCl stimulation elicited a clear response. This suggests that glucose sensitivity may have been hindered by the alginate encapsulation at the studied flow rate. A similar trend was observed in human islet perfusion experiments, where insulin secretion fluctuated unpredictably during glucose stimulation, likely due to residual glucose or amino acids from the culture media. Additionally, differences between suspension and encapsulated control groups further suggest that encapsulation impaired glucose sensing and insulin release despite preserved insulin content. To address these

challenges, optimizing the alginate composition, crosslinking density, and gelation method could enhance glucose diffusion while maintaining immunoprotection.

Porcine model implantation studies demonstrated that the devices could function as arterio-venous shunts, maintaining high flow rates and patency for seven days post-implantation. Notably, the devices exhibited minimal fibrosis and tissue growth on the external surface compared to control ePTFE grafts. Cell-laden devices also maintained perfusion with clear lumens during this period. However, short-term implantation studies are insufficient to assess long-term efficacy, as it remains unclear whether longer implantation periods would result in thrombosis and subsequent occlusion. Another issue encountered during the *in vivo* study was graft kinking due to the complex device geometry and limited space in the implant site. Two cell-free devices kinked during the study period, leading to graft occlusion. To mitigate this, an additional polymer sleeve could be added around the device to provide some structural integrity, or a better polymer or polymer composite could be developed to enhance vascular channel stiffness while retaining tensile strength and hemocompatibility. The use of non-diabetic porcine models was another limitation, as distinguishing human and porcine insulin in blood plasma is challenging, hindering an overall understanding of device functionality. Although maturation markers were detected in implanted cells, islet viability was suboptimal, likely due to the immune response against human SC-derived islet xenografts in the pig system. While alginate encapsulation demonstrated immunoprotective properties in rodent models, [80] further validation is required in human or non-human primates. However, given the modularity of our devices to accommodate various cells and matrix compositions, future studies could explore the use of better immunoprotective matrices or genetically engineered immune-evasive or immune-cloaked islets [25, 89] with vasculogenic matrices to enhance graft functionality.

4.2. Conclusion and future directions

This study presents a novel approach to addressing the challenges of T1D treatment by developing a macroencapsulation device with embedded vascular channels. By integrating pre-formed vascular structures, the device ensures immediate perfusion, mitigating hypoxia-related cell loss and improving mass transfer to encapsulated insulin-producing cells. *In vitro* studies demonstrated robust cell viability and function, with multi-channel designs showing enhanced insulin responsiveness compared to single-channel prototypes. *In vivo* experiments in a porcine model confirmed device patency, absence of thrombosis or fibrosis, and the sustained viability of encapsulated SC-islets. These findings validate the potential of this device as a promising platform for cell-based therapies in T1D treatment. In addition, this system also presents significant potential for *in vitro* applications beyond transplantation. By serving as a physiologically relevant platform to study human pancreas biology, drug screening and toxicity assessments that closely mimics *in vivo* conditions.

For future studies, testing in diabetic rat models for a long-term implant period should be conducted to evaluate glycemic control and insulin independence over extended durations. This will provide critical insights into the device's ability to maintain glucose homeostasis in a physiologically relevant diabetic environment. Further, the incorporation of supportive cells, such as MSCs or endothelial cells, may further improve vascularization and immune modulation. Additionally, incorporating immune-evasive or immune-cloaked cells along with vascularizing hydrogels could further enhance the survival and function of embedded cells by reducing immune recognition and promoting rapid vascular integration post-implantation. Further, to support clinical translation, it is essential to focus on scaling up fabrication processes while ensuring reproducibility and minimizing batch-to-batch variations.

5. References:

1. Atkinson, M.A., G.S. Eisenbarth, and A.W. Michels, *Type 1 diabetes.* Lancet, 2014. **383**(9911): p. 69-82.
2. von Scholten, B.J., et al., *Current and future therapies for type 1 diabetes.* Diabetologia, 2021. **64**(5): p. 1037-1048.
3. Notkins, A.L., *Immunologic and genetic factors in type 1 diabetes.* J Biol Chem, 2002. **277**(46): p. 43545-8.
4. Noble, J.A., *Immunogenetics of type 1 diabetes: A comprehensive review.* J Autoimmun, 2015. **64**: p. 101-12.
5. Langlois, A., et al., *Islet Transplantation: Current Limitations and Challenges for Successful Outcomes.* Cells, 2024. **13**(21).
6. Juang, J.H., et al., *Implanted islet mass influences the effects of dipeptidyl peptidase-IV inhibitor LAF237 on transplantation outcomes in diabetic mice.* Biomed J, 2021. **44**(6 Suppl 2): p. S210-S217.
7. Shapiro, A.M., M. Pokrywczynska, and C. Ricordi, *Clinical pancreatic islet transplantation.* Nat Rev Endocrinol, 2017. **13**(5): p. 268-277.
8. Ricordi, C., *Lilly Lecture 2002: Islet Transplantation: A Brave New World.* Diabetes, 2003. **52**(7): p. 1595-1603.
9. Tector, A.J., et al., *The Possible Role of Anti-Neu5Gc as an Obstacle in Xenotransplantation.* Front Immunol, 2020. **11**: p. 622.
10. Dai, Y., et al., *Targeted disruption of the α1,3-galactosyltransferase gene in cloned pigs.* Nature Biotechnology, 2002. **20**(3): p. 251-255.
11. Shin, J.S., et al., *Long-term control of diabetes in immunosuppressed nonhuman primates (NHP) by the transplantation of adult porcine islets.* Am J Transplant, 2015. **15**(11): p. 2837-50.
12. Reardon, S. <*First pig to human heart transplant what can scientists learn.pdf*>. 2022; Available from: https://www.nature.com/articles/d41586-022-00111-9.
13. Pagliuca, F.W., et al., *Generation of functional human pancreatic beta cells in vitro.* Cell, 2014. **159**(2): p. 428-39.
14. Kroon, E., et al., *Pancreatic endoderm derived from human embryonic stem cells generates glucose-responsive insulin-secreting cells in vivo.* Nat Biotechnol, 2008. **26**(4): p. 443-52.
15. Rezania, A., et al., *Reversal of diabetes with insulin-producing cells derived in vitro from human pluripotent stem cells.* Nat Biotechnol, 2014. **32**(11): p. 1121-33.
16. Russ, H.A., et al., *Controlled induction of human pancreatic progenitors produces functional beta-like cells in vitro.* EMBO J, 2015. **34**(13): p. 1759-72.
17. Wu, J., et al., *Treating a type 2 diabetic patient with impaired pancreatic islet function by personalized endoderm stem cell-derived islet tissue.* Cell Discov, 2024. **10**(1): p. 45.
18. Millman, J.R., et al., *Generation of stem cell-derived beta-cells from patients with type 1 diabetes.* Nat Commun, 2016. **7**: p. 11463.
19. Hogrebe, N.J., et al., *Targeting the cytoskeleton to direct pancreatic differentiation of human pluripotent stem cells.* Nat Biotechnol, 2020. **38**(4): p. 460-470.
20. Arroyave, F., Y. Uscategui, and F. Lizcano, *From iPSCs to Pancreatic beta Cells: Unveiling Molecular Pathways and Enhancements with Vitamin C and Retinoic Acid in Diabetes Research.* Int J Mol Sci, 2024. **25**(17).

21. Wang, S., et al., *Transplantation of chemically induced pluripotent stem-cell-derived islets under abdominal anterior rectus sheath in a type 1 diabetes patient.* Cell, 2024. **187**(22): p. 6152-6164 e18.
22. Ben-David, U. and N. Benvenisty, *The tumorigenicity of human embryonic and induced pluripotent stem cells.* Nat Rev Cancer, 2011. **11**(4): p. 268-77.
23. JDCA. *Vertex T1D Trial Paused After 2 Unrelated Patient Deaths*. 2024; Available from: https://www.thejdca.org/publications/report-library/archived-reports/2024-reports/vertex-t1d-trial-paused-after-2-unrelated-patient-deaths-crispr-collab-ends-next-day.html#:~:text=Vertex%20pauses%20VX%2D880%20T1D,with%20most%20being%20insulin%20independent.
24. Castro-Gutierrez, R., et al., *Protecting Stem Cell Derived Pancreatic Beta-Like Cells From Diabetogenic T Cell Recognition.* Front Endocrinol (Lausanne), 2021. **12**: p. 707881.
25. Yoshihara, E., et al., *Immune-evasive human islet-like organoids ameliorate diabetes.* Nature, 2020. **586**(7830): p. 606-611.
26. Skowera, A., et al., *CTLs are targeted to kill beta cells in patients with type 1 diabetes through recognition of a glucose-regulated preproinsulin epitope.* J Clin Invest, 2008. **118**(10): p. 3390-402.
27. Bisceglie, V., *Über die antineoplastische Immunität.* Zeitschrift für Krebsforschung, 1934. **40**(1): p. 122-140.
28. Lanza, R.P., W.M. Kühtreiber, and W.L. Chick, *Encapsulation technologies.* Tissue engineering, 1995. **1**(2): p. 181-196.
29. Desai, T. and L.D. Shea, *Advances in islet encapsulation technologies.* Nat Rev Drug Discov, 2017. **16**(5): p. 338-350.
30. Vaithilingam, V. and B.E. Tuch, *Islet transplantation and encapsulation: an update on recent developments.* Rev Diabet Stud, 2011. **8**(1): p. 51-67.
31. Scharp, D.W. and P. Marchetti, *Encapsulated islets for diabetes therapy: history, current progress, and critical issues requiring solution.* Adv Drug Deliv Rev, 2014. **67-68**: p. 35-73.
32. Omer, A., et al., *Long-term normoglycemia in rats receiving transplants with encapsulated islets.* Transplantation, 2005. **79**(1): p. 52-8.
33. Soon-Shiong, P., *Encapsulated islet cell therapy for the treatment of diabetes: Intraperitoneal injection of islets.* Journal of Controlled Release, 1996. **39**(2): p. 399-409.
34. Storrs, R., et al., *Preclinical development of the Islet Sheet.* Ann N Y Acad Sci, 2001. **944**(1): p. 252-66.
35. Dufrane, D., R.M. Goebbels, and P. Gianello, *Alginate macroencapsulation of pig islets allows correction of streptozotocin-induced diabetes in primates up to 6 months without immunosuppression.* Transplantation, 2010. **90**(10): p. 1054-62.
36. Gabr, M.M., et al., *Insulin-producing Cells from Adult Human Bone Marrow Mesenchymal Stromal Cells Could Control Chemically Induced Diabetes in Dogs: A Preliminary Study.* Cell Transplant, 2018. **27**(6): p. 937-947.
37. Ramzy, A., et al., *Implanted pluripotent stem-cell-derived pancreatic endoderm cells secrete glucose-responsive C-peptide in patients with type 1 diabetes.* Cell Stem Cell, 2021. **28**(12): p. 2047-2061 e5.
38. Brandon, E.P., et al., *Pluripotent Stem Cell–Derived Islet Replacement Therapy for Diabetes*, in *Second Generation Cell and Gene-based Therapies*. 2020. p. 157-181.

39. Magisson, J., et al., *Safety and function of a new pre-vascularized bioartificial pancreas in an allogeneic rat model.* J Tissue Eng, 2020. **11**: p. 2041731420924818.
40. Moure, A., et al., *Optimization of an O(2)-balanced bioartificial pancreas for type 1 diabetes using statistical design of experiment.* Sci Rep, 2022. **12**(1): p. 4681.
41. Carlsson, P.O., et al., *Transplantation of macroencapsulated human islets within the bioartificial pancreas betaAir to patients with type 1 diabetes mellitus.* Am J Transplant, 2018. **18**(7): p. 1735-1744.
42. Gholipourmalekabadi, M., et al., *Oxygen-Generating Biomaterials: A New, Viable Paradigm for Tissue Engineering?* Trends Biotechnol, 2016. **34**(12): p. 1010-1021.
43. Berman, D.M., et al., *Bioengineering the Endocrine Pancreas: Intraomental Islet Transplantation Within a Biologic Resorbable Scaffold.* Diabetes, 2016. **65**(5): p. 1350-61.
44. An, D., et al., *Designing a retrievable and scalable cell encapsulation device for potential treatment of type 1 diabetes.* Proceedings of the National Academy of Sciences, 2018. **115**(2): p. E263-E272.
45. Vaithilingam, V., et al., *Effect of alginate encapsulation on the cellular transcriptome of human islets.* Biomaterials, 2011. **32**(33): p. 8416-25.
46. Ashimova, A., et al., *Cell Encapsulation Within Alginate Microcapsules: Immunological Challenges and Outlook.* Front Bioeng Biotechnol, 2019. **7**: p. 380.
47. Elliott, R.B., et al., *Intraperitoneal alginate-encapsulated neonatal porcine islets in a placebo-controlled study with 16 diabetic cynomolgus primates.* Transplant Proc, 2005. **37**(8): p. 3505-8.
48. Espona-Noguera, A., et al., *Review of Advanced Hydrogel-Based Cell Encapsulation Systems for Insulin Delivery in Type 1 Diabetes Mellitus.* Pharmaceutics, 2019. **11**(11).
49. Jacobs-Tulleneers-Thevissen, D., et al., *Sustained function of alginate-encapsulated human islet cell implants in the peritoneal cavity of mice leading to a pilot study in a type 1 diabetic patient.* Diabetologia, 2013. **56**(7): p. 1605-14.
50. Buder, B., et al., *Encapsulated islet transplantation: strategies and clinical trials.* Immune Netw, 2013. **13**(6): p. 235-9.
51. Farina, M., et al., *Cell encapsulation: Overcoming barriers in cell transplantation in diabetes and beyond.* Adv Drug Deliv Rev, 2019. **139**: p. 92-115.
52. Calafiore, R., G. Basta, and P. Montanucci, *Microencapsulation of Islets for the Treatment of Type 1 Diabetes Mellitus (T1D)*, in *Cell Microencapsulation: Methods and Protocols*, E.C. Opara, Editor. 2017, Springer New York: New York, NY. p. 283-304.
53. Shih, H. and C.C. Lin, *Photoclick Hydrogels Prepared from Functionalized Cyclodextrin and Poly(ethylene glycol) for Drug Delivery and in Situ Cell Encapsulation.* Biomacromolecules, 2015. **16**(7): p. 1915-23.
54. Phelps, E.A., et al., *Maleimide cross-linked bioactive PEG hydrogel exhibits improved reaction kinetics and cross-linking for cell encapsulation and in situ delivery.* Adv Mater, 2012. **24**(1): p. 64-70, 2.
55. Teramura, Y. and H. Iwata, *Bioartificial pancreas microencapsulation and conformal coating of islet of Langerhans.* Adv Drug Deliv Rev, 2010. **62**(7-8): p. 827-40.
56. Yitayew, M.Y., et al., *An investigation of functionalized chitosan and alginate multilayer conformal nanocoating on mouse beta cell spheroids as a model for pancreatic islet transplantation.* Int J Biol Macromol, 2024. **278**(Pt 4): p. 134960.

57. Kizilel, S., et al., *Encapsulation of pancreatic islets within nano-thin functional polyethylene glycol coatings for enhanced insulin secretion.* Tissue Eng Part A, 2010. **16**(7): p. 2217-28.
58. Yang, H.K. and K.H. Yoon, *Current status of encapsulated islet transplantation.* J Diabetes Complications, 2015. **29**(5): p. 737-43.
59. Lanza, R.P., et al., *Xenotransplantation of canine, bovine, and porcine islets in diabetic rats without immunosuppression.* Proc Natl Acad Sci U S A, 1991. **88**(24): p. 11100-4.
60. Araki, Y., et al., *Biohybrid Artificial Pancreas Long-Term Insulin Secretion by Devices Seeded with Canine Islets.* Diabetes, 1985. **34**(9): p. 850-854.
61. Moyer, J.C., et al., *An arteriovenous mock circulatory loop and accompanying bond graph model for in vitro study of peripheral intravascular bioartificial organs.* Artif Organs, 2024. **48**(4): p. 336-346.
62. Yang, K., et al., *A therapeutic convection-enhanced macroencapsulation device for enhancing beta cell viability and insulin secretion.* Proc Natl Acad Sci U S A, 2021. **118**(37).
63. Song, S., et al., *An intravascular bioartificial pancreas device (iBAP) with silicon nanopore membranes (SNM) for islet encapsulation under convective mass transport.* Lab Chip, 2017. **17**(10): p. 1778-1792.
64. Han, E.X., et al., *Development of a Bioartificial Vascular Pancreas.* J Tissue Eng, 2021. **12**: p. 20417314211027714.
65. Richards, D., et al., *Photoresponsive Hydrogels with Photoswitchable Stiffness: Emerging Platforms to Study Temporal Aspects of Mesenchymal Stem Cell Responses to Extracellular Stiffness Regulation*, in *Cell Biology and Translational Medicine, Volume 5: Stem Cells: Translational Science to Therapy*, K. Turksen, Editor. 2019, Springer International Publishing: Cham. p. 53-69.
66. Lugano, R., M. Ramachandran, and A. Dimberg, *Tumor angiogenesis: causes, consequences, challenges and opportunities.* Cell Mol Life Sci, 2020. **77**(9): p. 1745-1770.
67. Brissova, M. and A.C. Powers, *Revascularization of transplanted islets: can it be improved?* Diabetes, 2008. **57**(9): p. 2269-71.
68. Marek-Trzonkowska, N., et al., *Therapy of type 1 diabetes with CD4(+)CD25(high)CD127-regulatory T cells prolongs survival of pancreatic islets - results of one year follow-up.* Clin Immunol, 2014. **153**(1): p. 23-30.
69. Cunha, J.P., et al., *Human multipotent adult progenitor cells enhance islet function and revascularisation when co-transplanted as a composite pellet in a mouse model of diabetes.* Diabetologia, 2017. **60**(1): p. 134-142.
70. Rackham, C.L., et al., *Co-transplantation of mesenchymal stem cells maintains islet organisation and morphology in mice.* Diabetologia, 2011. **54**(5): p. 1127-35.
71. Hogan, M.F. and R.L. Hull, *The islet endothelial cell: a novel contributor to beta cell secretory dysfunction in diabetes.* Diabetologia, 2017. **60**(6): p. 952-959.
72. Sun, X., Y. Aghazadeh, and S.S. Nunes, *Isolation of ready-made rat microvessels and its applications in effective in vivo vascularization and in angiogenic studies in vitro.* Nat Protoc, 2022. **17**(12): p. 2721-2738.
73. Aghazadeh, Y., et al., *Microvessels support engraftment and functionality of human islets and hESC-derived pancreatic progenitors in diabetes models.* Cell Stem Cell, 2021. **28**(11): p. 1936-1949 e8.

74. Balboa, D., et al., *Functional, metabolic and transcriptional maturation of human pancreatic islets derived from stem cells.* Nat Biotechnol, 2022. **40**(7): p. 1042-1055.
75. Gu, Y., et al., *Perioperative Outcomes: Polycarbonate Polyurethane Artificial Blood Vessel Versus Polyester Artificial Blood Vessel.* J Endovasc Ther, 2024: p. 15266028241283363.
76. Wijeyaratne, S.M. and L. Kannangara, *Safety and efficacy of electrospun polycarbonate-urethane vascular graft for early hemodialysis access: first clinical results in man.* J Vasc Access, 2011. **12**(1): p. 28-35.
77. Dong, X., et al., *Construction of a bilayered vascular graft with smooth internal surface for improved hemocompatibility and endothelial cell monolayer formation.* Biomaterials, 2018. **181**: p. 1-14.
78. Duvivier-Kali, V.r.F., et al., *Complete Protection of Islets Against Allorejection and Autoimmunity by a Simple Barium-Alginate Membrane.* Diabetes, 2001. **50**(8): p. 1698-1705.
79. Bochenek, M.A., et al., *Alginate encapsulation as long-term immune protection of allogeneic pancreatic islet cells transplanted into the omental bursa of macaques.* Nat Biomed Eng, 2018. **2**(11): p. 810-821.
80. Hoesli, C.A., et al., *Reversal of diabetes by betaTC3 cells encapsulated in alginate beads generated by emulsion and internal gelation.* J Biomed Mater Res B Appl Biomater, 2012. **100**(4): p. 1017-28.
81. Moeun, B.N., et al., *Oxygenation and function of endocrine bioartificial pancreatic tissue constructs under flow for preclinical optimization.* J Tissue Eng, 2025. **16**: p. 20417314241284826.
82. Weber, L.M., C.G. Lopez, and K.S. Anseth, *Effects of PEG hydrogel crosslinking density on protein diffusion and encapsulated islet survival and function.* J Biomed Mater Res A, 2009. **90**(3): p. 720-9.
83. MacRae, J.M., et al., *Arteriovenous Access Failure, Stenosis, and Thrombosis.* Can J Kidney Health Dis, 2016. **3**: p. 2054358116669126.
84. Calafiore, R., et al., *Human Stem Cell Therapy for the Cure of Type 1 Diabetes Mellitus (T1D): A Hurdle Course between Lights and Shadows.* Endocrines, 2024. **5**(4): p. 465-477.
85. Rodrigues Oliveira, S.M., et al., *Type 1 Diabetes Mellitus: A Review on Advances and Challenges in Creating Insulin Producing Devices.* Micromachines (Basel), 2023. **14**(1).
86. Hillberg, A.L., et al., *Improving alginate-poly-L-ornithine-alginate capsule biocompatibility through genipin crosslinking.* J Biomed Mater Res B Appl Biomater, 2013. **101**(2): p. 258-68.
87. EASD. *Islet allotransplantation into pre-vascularised Sernova Cell Pouch™: interim results*. 2024.
88. Zhu, H., et al., *Selection of Implantation Sites for Transplantation of Encapsulated Pancreatic Islets.* Tissue Eng Part B Rev, 2018. **24**(3): p. 191-214.
89. Harding, J., et al., *Immune-privileged tissues formed from immunologically cloaked mouse embryonic stem cells survive long term in allogeneic hosts.* Nat Biomed Eng, 2024. **8**(4): p. 427-442.